HIGH-FREQUENCY SPECTRA OF EARTHQUAKES AND EXPLOSIONS

F. J. Tanis

Environmental Research Institute of Michigan

Prepared for:

Air Force Office of Scientific Research

September 1973

AD 769 578

UNCLASSIFIED

SECURITY CLASSIFICATION OF THIS PAGE (When Data Entered)

REPORT DOCUMENTATION PAGE	READ INSTRUCTIONS BEFORE COMPLETING FORM
1. REPORT NUMBER: AFOSR - TR - 73 - 1986	2. GOVT ACCESSION NO. / 3. RECIPIENT'S CATALOG NUMBER
4. TITLE (and Subtitle): High-Frequency Spectra of Earthquakes and Explosions	5. TYPE OF REPORT & PERIOD COVERED: Final Report 1 June 1972 through 31 May 1973
	6. PERFORMING ORG. REPORT NUMBER: 192700-3-F
7. AUTHOR(s): F. J. Tanis	8. CONTRACT OR GRANT NUMBER(s): F44620-72-C-0077
9. PERFORMING ORGANIZATION NAME AND ADDRESS: Environmental Research Institute of Michigan, P. O. Box 618, Ann Arbor, MI 48107	10. PROGRAM ELEMENT, PROJECT, TASK AREA & WORK UNIT NUMBERS: ARPA Order No. 2134, Program Code No. F10
11. CONTROLLING OFFICE NAME AND ADDRESS: Director, Advanced Research Projects Agency, 1400 Wilson Boulevard, Arlington, VA 22209	12. REPORT DATE: September 1973
	13. NUMBER OF PAGES: 49
14. MONITORING AGENCY NAME AND ADDRESS (if different from Controlling Office): Air Force Office of Scientific Research/NPG, 1400 Wilson Boulevard, Arlington, VA 22209	15. SECURITY CLASS. (of this report): Unclassified
	15a. DECLASSIFICATION/DOWNGRADING SCHEDULE

16. DISTRIBUTION STATEMENT (of this Report)

Approved for public release; distribution unlimited.

17. DISTRIBUTION STATEMENT (of the abstract entered in Block 20, if different from Report)

18. SUPPLEMENTARY NOTES

19. KEY WORDS (Continue on reverse side if necessary and identify by block number)

Earthquake data
Explosion data
Near-field earthquake data
Coda spectral analysis
Body wave data
Path effect

20. ABSTRACT (Continue on reverse side if necessary and identify by block number)

Existing seismic earthquake and explosion data have been analyzed as part of the near-field earthquake program. Source characteristics of small magnitude events were investigated to better understand earthquake/explosion discrimination techniques.

Coda spectral analysis was found useful in determining source parameters from high-frequency data. Because of the large influence of path effect on spectral shape, the use of body wave data was found to present greater difficulties.

(Continued)

DD FORM 1 JAN 73 1473 EDITION OF 1 NOV 65 IS OBSOLETE

UNCLASSIFIED

SECURITY CLASSIFICATION OF THIS PAGE (When Data Entered)

1.

20.

Source parameters did not seem to be significantly different for explosions and earthquakes. Site location generally had a strong effect on source characteristics.

SUMMARY

The Geophysics Section of the Environmental Research Institute of Michigan's Infrared and Optics Division has analyzed existing seismic data as part of the near-field earthquake program. Our purpose was to investigate the source time function of small earthquakes to (1) better understand the explosion/earthquake magnitude discriminant $M_s:m_b$, and (2) define its lower limit of application. Since large earthquakes are considered to be the superposition of many smaller events, study of small earthquakes may be the key to understanding $M_s:m_b$.

Small earthquakes are dominated by high-frequency seismic waves, and existing field data includes the major portion (0.5 to 100 Hz) of spectral energy. Efforts have been therefore directed toward understanding the high-frequency spectrum. To this end, studies have examined body wave and seismic coda spectra.

The high-frequency spectrum is dramatically influenced by attenuation. Examination of many small earthquakes recorded in the 10 km to 100 km range revealed that no reliable information could generally be found higher than about 30 Hz. To gain information beyond 30 Hz it is necessary to record the data at very close ranges (less than 5 km) and use special pre-emphasis recording techniques. Calculation of small earthquake magnitudes from frequency spectra of explosions and earthquakes suggests that the $M_s:m_b$ criterion is limited by observable differences in M_s (i.e., for events of less than 2.5 magnitude).

An empirical technique has been applied to maximum seismic signals to reveal source spectra corner frequencies. Because of the difficulties in properly correcting for path effects, results show a large amount of scatter.

Analysis of the coda is based on a technique developed by Aki [1]. He found the coda spectrum to be independent of distance for short distances. A search of existing data has revealed a number of earthquake

---

1. Aki, K., Analysis of the Seismic Coda of Local Earthquakes as Scattered Waves, J. Geophys. Res., Vol. 74, No. 2, January 1969, pp. 614-631.

coda in a few selected areas.

Coda analysis was found to be a useful technique for determining source parameters from the high frequency spectra. Results are consistent with Aki's [2] ω-square spectrum scaling law as well as with reported dimension data [3].

In the limited range of available data ($0 < M_L < 2.5$), source spectra characteristics were not found to be useful for discriminating explosions and earthquakes. Furthermore, these results suggest that with the M_s:m_b criterion, m_b discrimination would not be effective for the above magnitude range.

---

2. Aki, K., Scaling Law of Earthquake Source Time-Function, Geophys. Journal Roy. Astro. Soc., Vol. 31, December 1972, pp. 3-25.

3. Wyss, M. and J. N. Brune, Seismic Moment, Stress, and Source Dimensions for Earthquakes in the California Nevada Region, J. Geophys. Res., Vol. 73, No. 14, July 1968.

PREFACE

The research described in this report was conducted by the Geophysics Section of the Environmental Research Institute of Michigan's Infrared and Optics Division. This work was performed under sponsorship of the Advanced Research Projects Agency and monitored by the Air Force Office of Scientific Research under Contract F44620-72-C-0077. The research period extended from 1 June 1972 through 31 May 1973. The Project Monitor was Donald W. Klick, Lt. Col. (USAF). The Principal Investigator was Mr. R. H. McLaughlin. The ERIM report number is 192700-3-F.

CONTENTS

Preceding page blank

ILLUSTRATIONS

HIGH-FREQUENCY SPECTRA OF EARTHQUAKES AND EXPLOSIONS

1
INTRODUCTION

A program to analyze existing earthquake and explosion data collected on previous field studies was initiated on 1 June 1972. The basic motive of this program, as a part of the near-field earthquake studies, is to analyze existing high-frequency seismograms of small earthquakes with magnitudes less than 4.0. Effort was directed toward better understanding of source mechanism and time functions. This program also evaluates possible discriminants for small earthquakes based on wave spectra and magnitude. The present report covers that work completed through 31 May 1973.

Source functions for earthquakes are not well understood. It is felt by many that the key to understanding earthquake source spectra is contained in the waves generated by small earthquakes. Large earthquakes may be multiple event sources and, if so, can be explained as the superposition of smaller events. Knowledge of the behavior of small earthquake seismic spectra, then, is crucial to evaluating the limitations of the $M_s:m_b$ discriminant technique.

The shape of the seismic spectrum is controlled by the source time-displacement history and degree of loss between source and station because of internal friction. It has been suggested that the source time function contributes in a major way to discrimination. While a simple impulse describes an explosion, a modified step function associated with dislocation is felt more appropriate for earthquakes. The far-field spectral content is sufficiently different to account for clear magnitude separation of explosions and earthquakes [4].

Savage (1972) and others have obtained relationships between the character of the source time displacement function and the far-field

---

4. SIPRI, Seismic Methods for Monitoring Underground Explosions, Stockholm International Peace Research Institute, Ed., D. Davies, 1971.

displacement spectra [5]. Typically, the low frequency portion of the latter can be approximated by a line parallel to the frequency axis. The high frequency trend is implied by the Fourier transform of the source time function and is inversely proportional to a power of frequency. The corner frequency is defined by the intersection of these two trends and behaves inversely with the pulse width of the displacement signal. Roughly this relation is equivalent to a corner frequency (Hz) inversely proportional to fault length (km). It seems reasonable, in this case, that a smaller pulse width would be associated with smaller earthquakes and higher corner frequencies. As this pulse width narrows, it approaches that representative of an explosion.

If we accept Aki's ω-square model and take m_b - 1.0 Hz, then an earthquake with $M_s < 2$ will appear as a point source [6]. The M_s:m_b criterion will obviously fail in this case unless there are substantial differences in the value of M_s for explosions and earthquakes. Neither the source time function nor the source finiteness is expected to cause amplitude spectral differences of Rayleigh waves between explosions and small earthquakes; rather, the source mechanism and focal depth are responsible for such differences (Aki, [7]). Thus it seems that small shallow earthquakes cannot be discriminated from comparable explosions.

In this program such spectral characteristics as corner frequency are examined using a coda analysis technique for small events. Behavior is related to the M_s:m_b criterion as applied to small earthquakes.

---

5. Savage, J. C., Relation of Corner Frequency to Fault Dimensions, J. Geophys. Res., Vol. 77, No. 20, July 1972, pp. 3788-3795.

6. Aki, K., Theoretical $M_s - m_b$ Relation for Small Magnitudes, Woods Hole Conference on Seismic Discrimination, Ed., J. F. Evernden, Vol. 1, July 1970, pp. 57-70.

7. Aki, K. and Y-B Tsai, Amplitude Spectra of Surface Waves From Small Earthquakes and Underground Nuclear Explosions, Woods Hole Conference on Seismic Discrimination, Ed., J. F. Evernden, Vol. 1, July 1970, pp. 291-328.

2
EXISTING SMALL EARTHQUAKE AND EXPLOSION DATA

2.1. EARTHQUAKE AND EXPLOSION SEISMIC RECORDINGS

During past field programs conducted by the Geophysics Laboratory, a large number of earthquake and explosion events were recorded on magnetic tape. Seismograms analyzed for this near-field earthquake program have been selected from this collection of records.

Earthquakes were largely recorded in southwestern United States and at several foreign stations. Field programs recording explosive sources, other than NTS events, have been limited to the eastern United States. All events considered in this program have magnitudes less than 4.5 and range primarily between 1.0 and 3.0 in magnitude. A major portion of the microearthquake events were recorded at less than 200 km distance. A representative list of sites and the number of events recorded is given in Table 1.

Many of the explosion field programs used several recording sites usually placed in line for purposes of refraction analysis. Aside from the NTS events and quarry shots, most recorded seismograms were obtained from underwater explosions of several tons TNT. Timing and shot position are known with great precision. Explosion data were recorded on magnetic tape from three-component Hall-Sears (Model HS-10) two-cycle geophones. In some early work only a single vertical HS-10 or a 2-cycle Willmore seismometer was used.

Earthquake field recordings, with only a few exceptions, were made at single stations. Origin times and approximate distance to the focus must be inferred from standard Gutenberg travel-time curves from the S-P residual. A good portion of these records were obtained using the HS-10 three-component package. Most of the earthquakes recorded in California were obtained using a 2-cycle Willmore geophone. (No long-period geophones have been used in connection with near source field work.)

2.2. HIGH-FREQUENCY SEISMIC SPECTRA

The high-frequency spectra of earthquake seismic signals are

TABLE 1. PARTIAL LISTING OF SMALL EARTHQUAKES AND EXPLOSION RECORDINGS

Site	Year Recorded	Event Type	Instrumentation	Quantity	Distance (km)
Shepard, Montana	1960	Earthquake	2-cycle vertical Willmore	20	80 - 250
Hollister, California	1961	Earthquake	2-cycle vertical Willmore	50	10 - 75
Hollister, California	1959	Earthquake	2-cycle vertical Willmore	43	10 - 225
Peterson's Ranch, California	1961	Earthquake	2-cycle vertical Willmore	13	5 - 75
Berry Creek, Nevada	1963	Explosion	3-component HS-10	22	25 - 35
Mauna Loa, Hawaii	1962	Earthquake	2-cycle vertical Willmore	25	10 - 60
Kau Desert, Hawaii	1962	Earthquake	2-cycle vertical Willmore	14	10 - 35
Mt. Laguna, California	1961	Earthquake	3-component HS-10	25	33 - 150
Mt. Laguna, California	1961	Explosion	3-component HS-10	10	95 - 200
American Samoa	1962	Earthquake	3-component HS-10	17	70 - 700
Crete	1962	Earthquake	3-component HS-10	26	14 - 400
Concepción, Chile	1962	Earthquake	3-component HS-10	36	24 - 310
Quetta, Pakistan	1962	Earthquake	3-component HS-10	14	10 - 900
Rincon, Puerto Rico	1962	Earthquake	3-component HS-10	20	13 - 200
Offshore, North Carolina	1962	Explosion	3-component HS-10	15	27 - 250
Lake Superior	1963	Explosion	3-component HS-10	82	10 - 300
Fibora Quarry, Michigan	1962	Explosion	3-component HS-10	31	54 - 218
Hendrick's Quarry, Michigan	1959	Explosion	3-component HS-10	29	75 - 200

shaped by the source spectrum parameters (e.g., stress drop, corner frequency), the degree of loss by internal friction (attenuation), and the field recording system response. Generally, field stations have been instrumented with a recording system having a flat velocity response to 100 Hz. Shape, then, is actually limited only by the first two factors. Any technique designed to gain source information from body and surface wave spectra must contend with rapid loss of high frequencies over short distances. Because of the high loss rate, spectra studies are almost always limited to records which have an (S-P) distance of less than 100 km and preferably less than 50 km.

The spectral shape of a typical earthquake seismogram shows a strong decreasing trend (usually 30 to 40 db/decade) for the higher frequencies. While this may be partially the result of source spectrum trends, it is probably mostly caused by attenuation. A gradual change from the strong decreasing trend to a flat portion is the result of decreasing signal-to-noise ratio.

Three-component one-third-octave particle velocity spectra for a small Chilean earthquake are shown in Fig. 1. This spectral shape seems typical of the data.

Cursory examination of records from several areas indicates that useful spectra data are generally limited on the high end to 30 or 40 Hz by natural background and electrically generated 60 Hz noise. One-third-octave high frequency analyses (to 100 Hz) were run for several earthquakes which appeared from the records to contain information not limited by background noise. A few instances were found where the very high frequency data (40 Hz and higher) could be attributed to earthquake seismics. However, in most cases, the high frequency levels look suspiciously influenced by broadband amplifier clipping or malfunction.

In summary, the earthquake data analyzed show that very few events in the range of 10 km to 100 km generate sufficiently high frequencies beyond 30 Hz to be adequately recorded above background levels. The high frequency trend, because of attenuation and/or source spectrum shape, is usually well established by 30 Hz. If corner frequency is

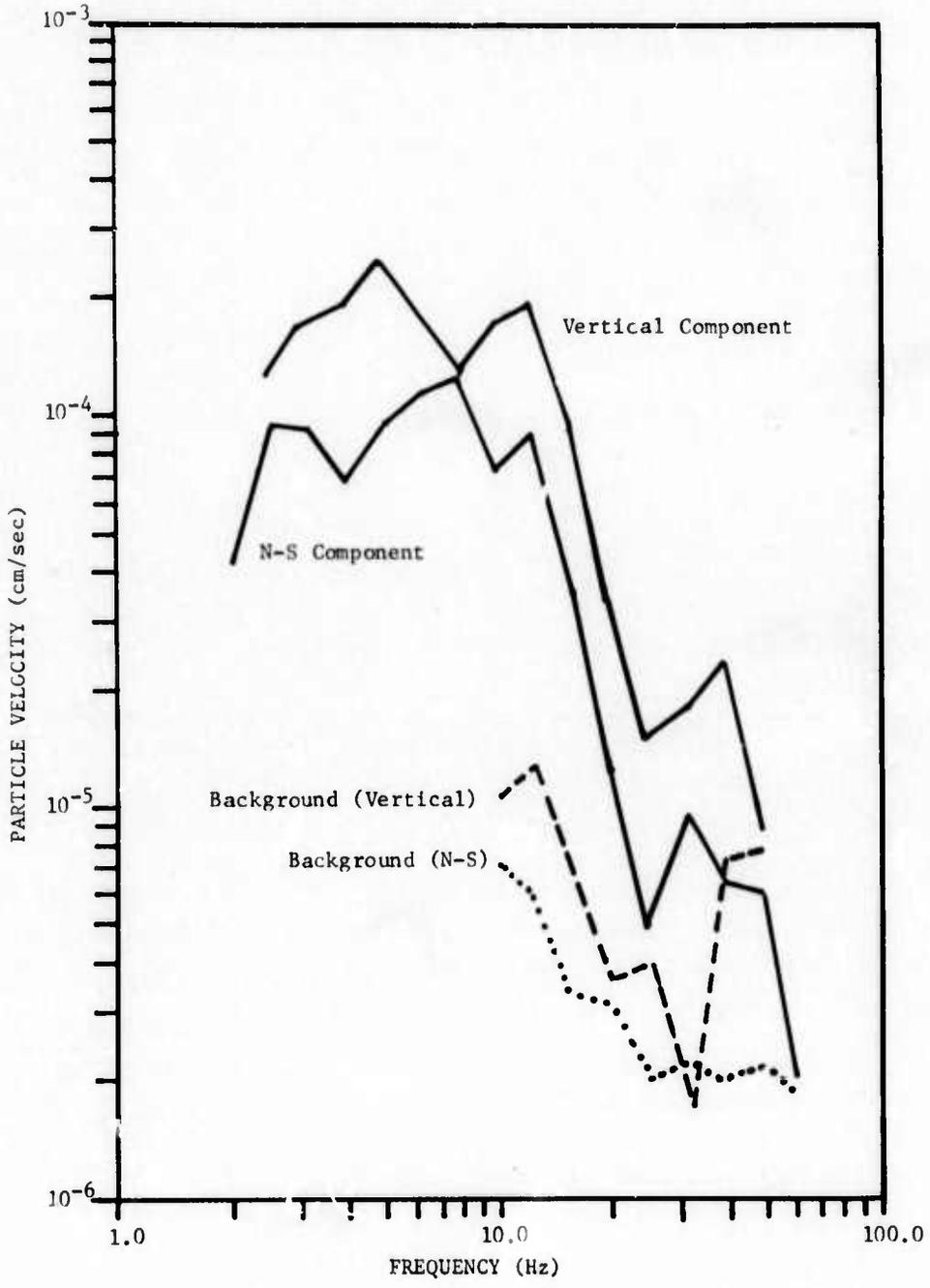

FIGURE 1. CHILEAN EARTHQUAKE, PARTICLE VELOCITY SPECTRA FOR MAXIMUM SIGNAL. (S-P Distance equals 50 km. Approximate M_L magnitude equals 1.7.

higher than 15 or 20 Hz, it is not likely to be resolved by our existing earthquake data.

2.3. SMALL EARTHQUAKE/EXPLOSION MAGNITUDES

Proponents of the M_s:m_b criterion have two important concerns: lower magnitude bands for earthquake/explosion separation, and thresholds for M_s, m_b determination. The question of minimum M_s determination cannot be studied since our data is exclusively high frequency. It has been projected however, that with improved instrumentation deployed at sites of low background noise level, an M_s magnitude of 2.8 should be detectable at teleseismic distances [4]. The results from a study by Thirlaway indicated that M_s:m_b lines are not convergent below magnitude 4.0 for explosions and earthquakes [8]. Basham on the other hand showed converging lines for small magnitudes [9].

In order to get some feeling for the behavior of small earthquake and explosion magnitudes, we applied a local magnitude scale developed by Richter [10]. This scale was developed for use in southern California with the Wood-Anderson torsional seismometer. For application of Richter's scale, the instrument has a natural period of 0.8 second, damping of 0.8, and magnification of 2800.

The local magnitude equation given by Richter is:

$$M_L = \log_{10}A - \log_{10}A_0$$

where A_0 is the maximum (zero to peak) trace deflection (on the Wood-Anderson) by an earthquake of magnitude zero and A is the maximum trace deflection of the earthquake whose magnitude is to be determined. The

---

8. Thirlaway, H. I. S., SIPRI, Seismic Methods for Monitoring Underground Explosions, Stockholm International Peace Research Institute, 1968, p. 63.

9. Basham, P. W., SIPRI, Seismic Methods for Monitoring Underground Explosions, Stockholm International Peace Research Institute, 1968, p. 67.

10. Richter, C. F., An Instrumental Magnitude Scale, Bull. Seism. Soc. Am., Vol. 25, 1935, pp. 1-32.

$\log_{10}A_0$ correction term is given by Richter as a function of distance for southern California. The scale has been worked out for distances up to 600 km. For distances less than 200 km it is perhaps the only practical scale available. Since our program is concentrating on events which are generally less than 100 km, such a magnitude measurement seems useful. Two assumptions must be made in order to apply Richter's M_L:

1. The Richter M_L correction for distance ($\log A_0$) has at least the same shape at locations other than southern California. Our single-station recording sites limit any possibility of calibrating an earthquake area for magnitude correction.

2. The local magnitude can be measured from spectra level at a fixed period of any seismometer when the Wood-Anderson is not available.

For purposes of computing magnitude the Richter correction for distance was applied to the largest amplitude after the P phases. Almost without exception this is the maximum trace amplitude. Amplitudes were taken from the one-third-octave frequency spectra at 5 Hz and converted to trace deflection on the Wood-Anderson system. Trace amplitude may be estimated from the filter output by applying an appropriate correction based on bandwidth. Conversion is accomplished by first estimating ground displacement from particle velocity spectra corrected for system gains. Trace deflection on the Wood-Anderson system was obtained using standard response curves and magnifications. The 5.0 Hz value was felt for these data to be least affected by changing earthquake source size. The maximum signal for many records of small earthquakes ($1.0 < M_L < 30$) resulted from a shear wave.

A second magnitude determination was made for the maximum of the P wave according to the formula

$$m_{bL} = \log_{10}A/T + D$$

where A equals the spectra level at 5.0 Hz and D equals a correction

for distance. For lack of any other distance correction, D was taken as the Richter correction for M_L, (i.e., $-\log_{10}A_0$). For this reason the notation m_{bL} is used. Although the unified magnitude correction is usually applied in m_b determinations, it is applicable only at much greater distances than 100 km. Before taking the log A/T the ground displacement was converted to corresponding trace displacement on the Wood-Anderson. These two magnitudes were computed for a number of earthquakes and small explosions for a wide variety of sites (see Tables 2 and 3). A plot of m_{bL} versus M_L is shown in Fig. 2. The points generally fall on the line obtained by Basham for earthquakes using the standard M_s and m_b magnitudes [9]. The scatter seems surprisingly low in view of the variety of sites and measurement at constant period. Explosion points are generally above the line, as would be expected since they tend to generate relatively smaller shear and surface waves. The separation does not, however, approach that experienced by Basham and others at magnitudes of 4.0 and greater. The effect of a shift in the ($-\log A_0$) distance correction factor will, because it is applied to both magnitudes, only tend to move points along an $m_{bL} = M_L + D$ line which perhaps more closely approximates this point trend.

The use of high frequency 5.0 Hz body wave and surface wave magnitudes does not appear to be useful, in view of the above data, for discrimination of explosions and earthquakes. Further, because of the similarity between M_s and M_L and m_b and m_{bL}, these data suggest that the M_s, m_b discriminant is not likely to work well for such small magnitudes.

A correction in our magnitude calculation technique has changed those values reported in Tables 2 and 3 from those previously reported [11].

---

11. Tanis, F. J., High-Frequency Spectra of Earthquakes and Explosions, Semi-Annual Informal Technical Report Number 192700-2-T, Environmental Research Institute of Michigan, Ann Arbor, February 1973.

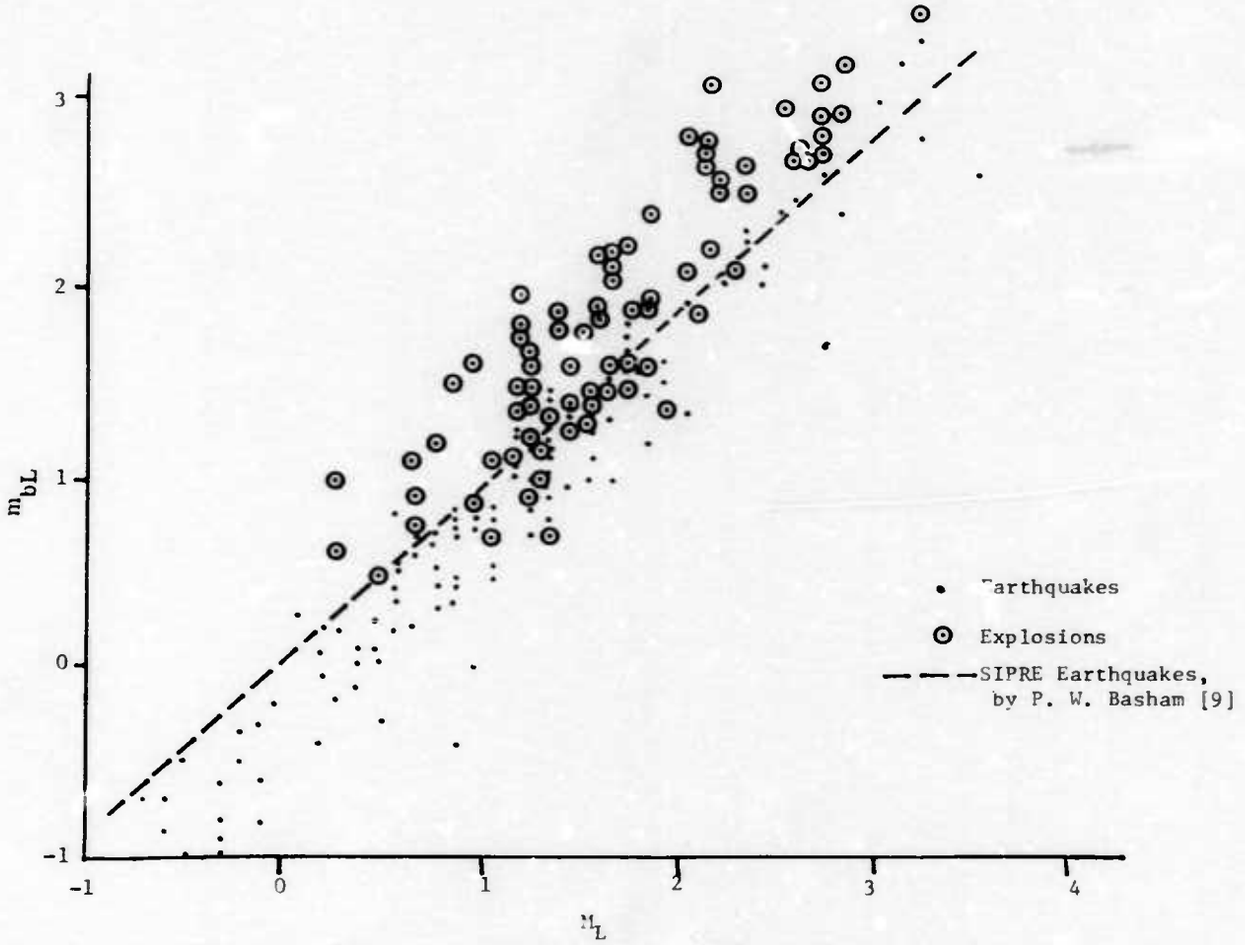

FIGURE 2. BODY WAVE MAGNITUDE m_{bL} VERSUS LOCAL MAGNITUDE M_L FOR EARTHQUAKES AND EXPLOSIONS

TABLE 2. SMALL EXPLOSION MAGNITUDES
(PLOTTED IN FIG. 2)

Distance (km)	M_L	m_{bL}	Distance (km)	M_L	m_{bL}
		Knife River, Minnesota, Lake Superior Underwater Series, 1963			
101.0	2.3	2.7	19.2	2.2	1.9
89.7	1.8	2.1	36.6	1.5	1.3
71.9	1.6	1.4	56.3	1.2	1.1
		Copper Harbor, Michigan Lake Superior Underwater Series, 1963			
10.4	0.7	0.9	96.7	1.5	1.8
66.6	1.4	1.6	105.0	1.6	1.5
154.0	1.4	1.5	34.2	1.8	2.2
127.0	1.3	1.4	18.7	1.4	1.0
120.0	1.3	1.8	53.8	1.6	1.3
56.5	1.4	1.2	89.5	1.4	1.5
46.5	1.0	1.6	105.0	1.3	1.5
39.1	1.6	1.8	93.3	1.3	1.8
43.5	1.3	1.2	85.7	1.5	1.9
125.0	1.7	1.9	79.5	1.9	1.9
70.4	0.7	1.1	119.0	2.4	2.1
76.7	1.3	2.0	119.0	1.7	1.5
		Upper Peninsula, Michigan Early Rise Series, 1966			
44.3	2.0	2.4	94.5	1.7	2.2
53.3	1.7	1.9	116.5	2.3	3.9
53.3	1.8	2.1	141.3	2.2	2.8
68.8	1.8	2.2			
		Fiborn Quarry, Michigan, 1962			
70.2	1.7	1.6	94.8	0.3	0.6
70.2	0.9	1.5	70.2	0.3	1.0

Table 2 (Cont.)

Distance (km)	M_L	m_{bL}	Distance (km)	M_L	m_{bL}
		Hendrick's Quarry, Michigan, 1962			
85.6	0.8	1.2	85.6	1.1	1.1
106.6	0.5	0.5	85.7	1.2	1.1
156.6	1.4	1.4	98.8	2.0	1.4
156.6	1.1	0.7	98.8	1.9	1.7
156.6	1.8	1.5			
		Union Furnace, Pennsylvania, 1959			
37.7	1.3	0.9	48.5	1.3	1.2
		St. Lawrence Seaway, 1958			
100.0	1.8	1.6	16.0	1.4	0.7
		Southern California, Hydra II, 1961			
123.0	1.3	1.4	123.0	2.8	2.8
123.0	2.1	2.1	123.0	2.7	2.7
180.0	1.5	1.6	123.0	2.4	2.5
		Carolina Coast, N. C. Offshore Shot Series, 1962			
107.0	2.3	2.5	159.0	2.2	2.2
127.0	3.3	3.5	197.0	2.7	2.7
152.0	2.5	2.7	156.0	2.2	2.7
163.0	2.8	2.9	192.0	2.9	3.2
232.0	2.7	2.7	151.0	2.4	2.7
249.0	2.3	2.1	189.0	2.8	3.1
226.0	2.9	2.9	166.0	2.2	2.8
250.0	2.6	2.4	148.0	2.5	2.7
233.0	1.3	1.7	27.0	0.7	0.7
171.0	1.8	2.2	36.0	1.5	1.3
206.0	2.8	2.7	39.0	1.0	0.8
199.0	2.6	3.0	42.0	1.3	0.9

TABLE 3. SMALL EARTHQUAKE MAGNITUDES
(PLOTTED IN FIG. 2)

Distance (km)	M_L	m_{bL}	Distance (km)	M_L	m_{bL}
		Kau Desert, Hawaii, 1962			
32.0	1.6	1.3	13.0	0.7	0.6
13.0	1.5	1.3	32.0	0.7	0.3
60.0	1.5	1.4	21.0	0.6	0.2
32.0	1.4	1.1	15.0	0.6	0.4
31.0	1.2	1.0	17.0	0.6	0.5
29.0	0.9	0.8	45.0	0.6	0.5
11.0	0.9	0.4	25.0	0.3	0.2
15.0	0.8	0.5	20.0	-0.2	-0.7
		Crete, Greece, 1962			
167.0	1.9	1.9	60.0	1.2	1.0
355.0	1.8	1.8	87.0	1.3	1.0
76.0	1.8	1.8	57.0	1.4	0.8
89.0	1.8	1.6	87.0	1.1	0.9
142.0	1.8	1.5	150.0	1.1	0.8
87.0	1.7	1.6	68.0	1.1	0.5
116.0	1.7	1.3	76.0	1.1	0.4
128.0	1.4	1.4	87.0	0.9	0.8
140.0	1.5	1.2	87.0	0.8	0.6
78.0	1.4	1.2	52.0	0.9	0.4
144.0	1.3	1.1	68.0	0.7	0.7
			402.0	3.2	3.2
		Pago Pago, American Samoa, 1962			
700.0	3.9	3.9	185.0	2.4	2.3
390.0	3.3	3.3	200.0	2.5	2.0
315.0	3.1	2.0	220.0	2.6	1.7
190.0	3.3	2.8	145.0	2.0	1.6
200.0	3.6	2.6	10.0	2.0	1.5
140.0	2.7	2.7	74.0	0.5	0.1

Table 3 (Cont.)

Distance (km)	M_L	m_{bL}	Distance (km)	M_L	m_{bL}
		Concepción, Chile, 1962			
310.0	2.9	2.4	29.0	0.6	0.9
103.0	2.4	2.4	37.0	0.4	0
115.0	1.8	2.6	47.0	0.2	0
50.0	2.0	1.4	29.0	-0.1	-0.6
127.0	1.4	0.1	29.0	-0.1	-0.8
140.0	1.4	1.0	29.0	-0.3	-0.8
85.0	1.4	0.9	24.0	-0.3	-0.9
115.0	1.1	0.8	24.0	-0.5	-1.0
		Hollister, California, 1961			
40.0	2.1	1.9	10.0	0.2	0.2
45.0	0.6	0.8	445.0	0.2	0.1
62.0	0.8	0.7	50.0	0.3	-0.2
60.0	0.9	0.4	24.0	0.1	0.2
3.0	0.8	0.4	10.0	0	-0.2
40.0	0.8	0.3	20.0	-0.2	-0.4
10.0	1.0	0	20.0	-0.5	-0.5
30.0	0.9	0.4	30.0	-0.4	-0.7
20.0	0.5	0.2	10.0	-0.3	-0.9
38.0	0.5	0	21.0	-0.6	-0.7
24.0	0.4	0.1	22.0	-0.7	-0.7
11.0	0.4	-0.1			
		Mt. Laguna, California, 1961			
27.0	-0.3	-0.6	93.0	1.4	0.9
29.0	-0.1	-0.3	100.0	1.5	1.0
36.0	0.2	-0.4	125.0	1.6	1.2
33.0	0.5	-0.3	144.0	1.6	1.1
127.0	0.9	0.7	147.0	1.6	1.0
65.0	0.9	0.9	81.0	1.7	1.0
94.0	1.0	0.7	127.0	1.9	1.7
91.0	1.2	1.2	90.0	1.9	1.4
23.0	1.2	1.2	81.0	1.9	1.2
85.0	1.4	1.4	33.0	2.3	2.0
101.0	1.3	0.8	123.0	2.5	2.1
96.0	1.3	0.7			

Total number of earthquakes: 113

Values of M_L cited elsewhere in this report are based on peak displacement spectral levels. Our technique of M_L determination was checked for consistency using NTS explosion data reported by Bayer [12]. Local magnitudes determined from particle velocities (from a NGC-21 seismometer) showed good agreement with those obtained directly from the Wood-Anderson seismometers.

3
ANALYSIS FOR SEISMIC SOURCE PARAMETERS

For the most part this study has examined microearthquakes for such spectral characteristics as corner frequency (or source dimension). Because of the limitation to a single station data, determination of radiation patterns and fault motions are not possible. The corner frequency, however, can give insight into the lower magnitude limits for m_b discriminants. Two separate approaches have been taken to analyze the seismic data for corner frequency. The first analyzes the coda portion whose size is dependent on magnitude and whose relative spectral shapes can be used to determine corner frequency. A second approach attempts to reveal corner frequency from the shear wave spectra by removing the implied shape effect of attenuation.

3.1. ANALYSIS OF EARTHQUAKE SEISMIC CODA

A technique for analysis of the coda to reveal source information was developed by Aki [1]. It is upon his work that this study is largely based. The coda is comprised of the numerous backscatter waves (surface waves) because of the elastic lateral heterogeneity. Coda may be regarded as the sum of many small independent events which are assumed to occur uniformly over a large area. The number of backscatters decreases exponentially with elapsed time. For distances less than 100 km, Aki found the degree of coda excitation to be independent

---

12. Bayer, K. C. and G. M. Wuollet, A Magnitude Yield Evaluation of Nuclear Events and One Chemical Explosion on the Nevada Test Site, U.S.G.S. Unpublished Report, July 1973.

of epicenter distance. P and S waves, on the other hand, can show strong variation as a result of path differences. The coda spectrum is only a function of time measured from the earthquake's origin time.

Earthquake coda were recorded during several field programs, especially when double-gaining was practiced. Seismic records with useful coda usually have "pinned" the amplifier during the body and early surface phases. However, in some instances full recorded records produced an acceptable coda. Aki found a strong dependence of the coda spectra on the geology of the station site. Therefore, coda analysis requires the use of a number of records obtained at a single station. We found our data quite suitable to coda analysis because we have data for several foreign sites and at least one United States site where large numbers (30-50) of small earthquakes were recorded. For each site, several events can be expected to be overrecorded.

The station spectrum $F(\omega/t)$ is directly related to the source spectrum $S(\omega)$ by correction factor $K(\omega/t)$ which accounts for all backscatter path effects such as attenuation and geometrical spreading for each station locality.

$$F(\omega/t) = |S(\omega)|\ K(\omega/t).$$

The decay $K(\omega/t)$ is actually equal to $|\phi\ (\omega/r_0)|$ times attenuation and geometrical spreading factors; $|\phi(\omega/r_0)|$ is a function of frequency only and expresses the absolute value of the Fourier transform of displacement from secondary waves generated at a scatter distance r_0. The source is taken with unit moment located at the same distance R from the scatterer. It is assumed that $R \simeq r_0 >>$ station/source distance. Aki found little variation in $\phi(\omega/r_0)$ with frequency. Thus normalization of the coda spectra to a zero time reference produces results which are within constant proportion to the source spectra [1].

Spectral analysis of the coda waves consists of running one-third-octave frequency passes from 1.0 Hz to 50 Hz. Signal levels are read at 1- or 2-second intervals after an elapsed time (t_e) of approximately $t_{0-P} + 2t_{(S-P)}$, or simply after all major Rayleigh waves pass. Usually about 20 seconds of coda signal is readable. Particle

velocities are converted to displacements and plotted on semi-log paper. Twenty seconds time is usually sufficient to establish the shape of exponential decay with time. Examples of these coda lines for Chile and California stations are shown in Figs. 3 and 4. There are sets of such lines for each of the one-third-octave frequencies.

Coda spectra were adjusted to zero time using the coda lines and an estimate of the zero to first onset time. As mentioned, this coda analysis was applied to a group of earthquakes and explosions within a range of 130 km from the source. Typical upper crust velocities were assumed to hold within this range, i.e., with P velocity of 6.1 km/sec and S velocity of 3.5 km/sec [13]. Using these velocities one obtains:

$$t_{0-P} = 1.35\ t_{S-P}$$

$$\Delta(\text{km}) = 8.25\ t_{S-P}\ (\text{sec})$$

where t_{0-P} is the time for the arrival of the P wave, t_{S-P} is the time between the arrival of P and S, and Δ is the distance to the source. Using these relations between S-P time and 0-P time, we adjusted coda readings to time after origin time.

When the coda of the earthquakes or explosions of one area were compared, they were remarkably similar in slope, though there was a considerable variation in the intercepts. A mean slope was determined for each group of explosions or earthquakes in one area. The intercept (i.e., the displacement at time zero) of the coda for each individual earthquake of the group was found by extrapolating a line with the mean slope through the midpoint of the displacement time curve for that earthquake. The normalized coda spectra is then a collection of these extrapolations for all readable frequencies. It was not generally possible to take coda readings beyond frequencies of 25 Hz. The inverse attenuation applied in the zero time adjustment is evident when comparing spectra adjusted to later times. Figure 5 suggests that coda spectra are being adjusted appropriately. Earthquake and explosion coda spectra were obtained from data recorded at the following sites:

---

13. Clark, S. P., Ed., Handbook of Physical Constants, Geological Society of America, Memoir 97, 1966.

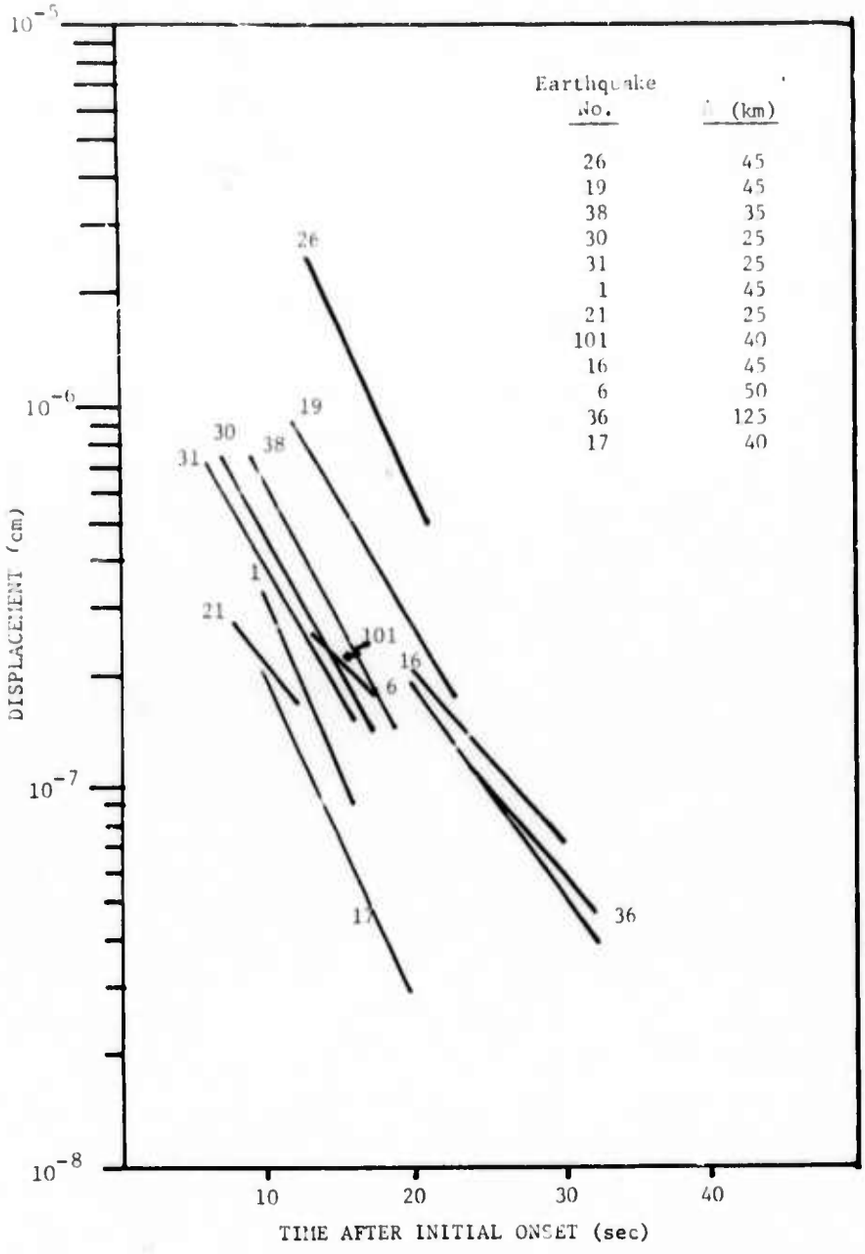

FIGURE 3. EARTHQUAKE CODA DISPLACEMENT VERSUS TIME AFTER ONSET IN A ONE-THIRD-OCTAVE BAND AT 10.0 Hz. Earthquake recorded at Hollister, California.

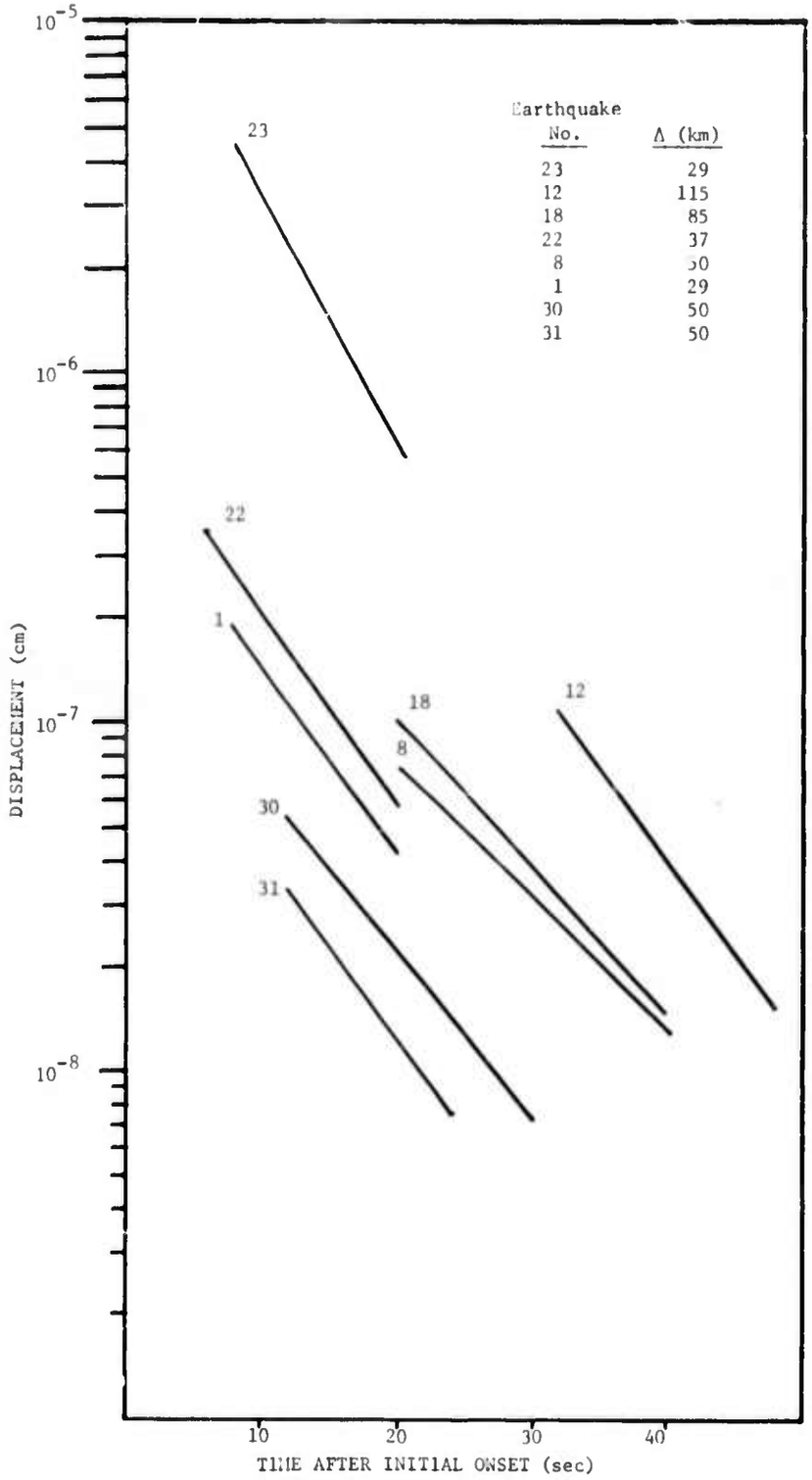

FIGURE 4. EARTHQUAKE CODA DISPLACEMENT VERSUS TIME IN A 10 Hz ONE-THIRD-OCTAVE BAND. Earthquakes recorded at Concepción, Chile.

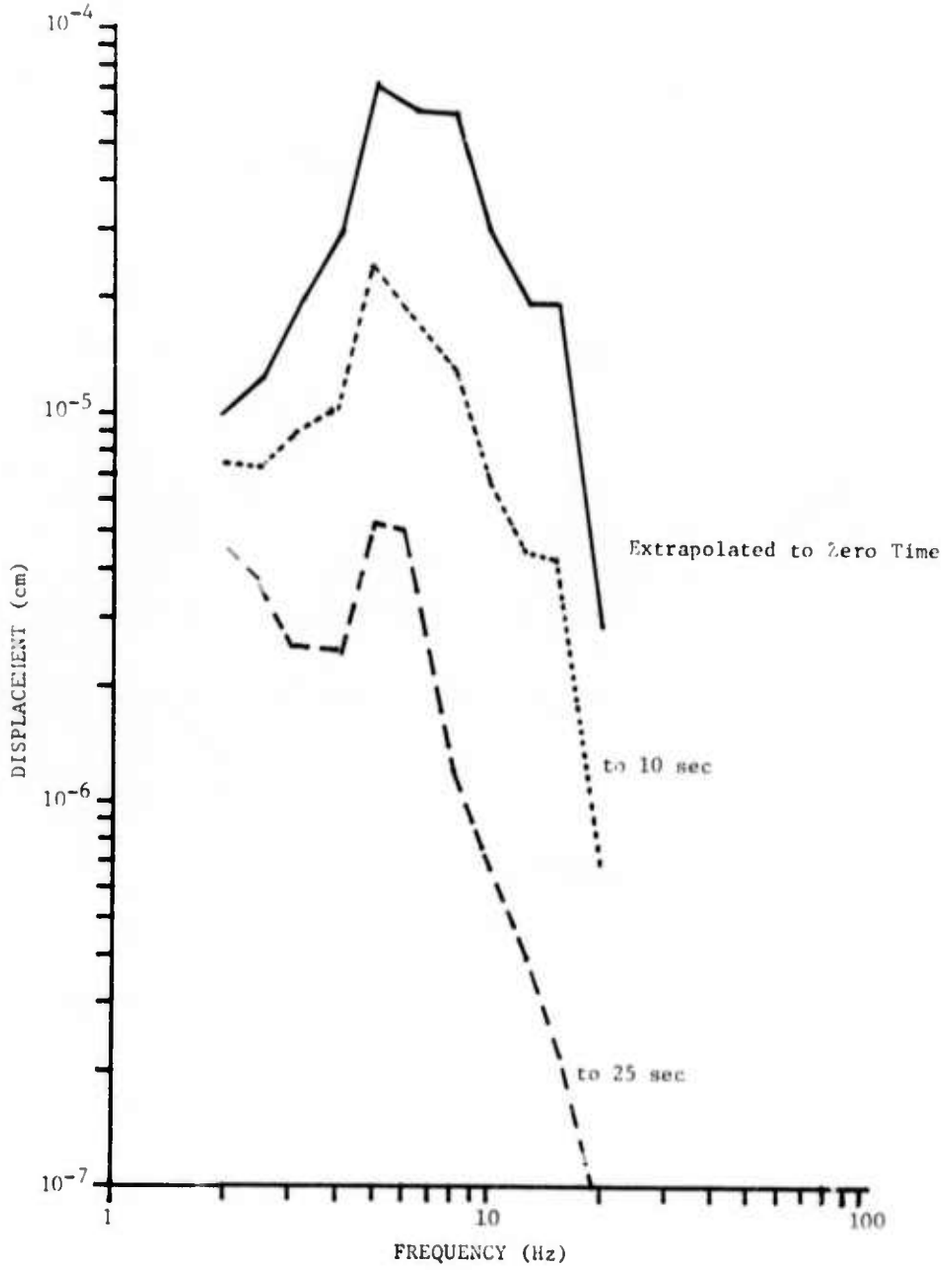

FIGURE 5. COMPARISON OF EXTRAPOLATED SPECTRAL SHAPES AT 0, 10, AND 25 SECONDS ELAPSED TIME. Earthquake recorded at Mauna Loa, Hawaii.

1. Concepción, Chile
2. Mauna Loa, Hawaii
3. Hollister, California
4. Berry Creek, Nevada
5. NTS, Mercury, Nevada

For all other sites in Table 1, pronounced coda were either not detected or appeared in insufficient number. Individual coda spectra for these areas are presented in Figs. 6, 7, and 8. Their shapes, and thereby source parameters, seem to vary dramatically from area to area but show strong similarities within each site. The normalized coda spectra reflect actual source spectra and as such contain information on the source dimension and size. Earthquake/explosion magnitude and source spectral characteristics are given in Table 4. Local magnitudes were obtained from the maximum shear or surface wave as discussed.

3.2. INTERPRETATION OF SEISMIC CODA SPECTRA

At this point an interpretation of the derived seismic spectra in terms of the seismic source is desirable. There is, however, no universally accepted definition of the far-field spectra in relation to the source. A number of models and corresponding spectra have been proposed. With different approaches, Randall [14] and Archembeau [15] have considered the relaxation of an initially stressed spherical inclusion within an unstressed medium. With these models they have derived a theoretical spectrum peaked at a frequency related to the seismic source dimension. (Randall, in a correction to the work of Archembeau, has recently shown that their model yields equivalent results [16].) Brune deals with a circular fault with a shear dislocation and finds

---

14. Randall, M. J., Seismic Radiation from a Sudden Phase Transition, J. Geophys. Res., Vol. 71, 1966, pp. 5297-5302.

15. Archembeau, C. B., General Theory of Elastodynamic Source Fields, Review of Geophysics, Vol. 6, 1968, pp. 241-287.

16. Randall, M. J., Spectral Peaks and Earthquake Source Dimension, J. Geophys. Res., Vol. 78, No. 14, May 1973.

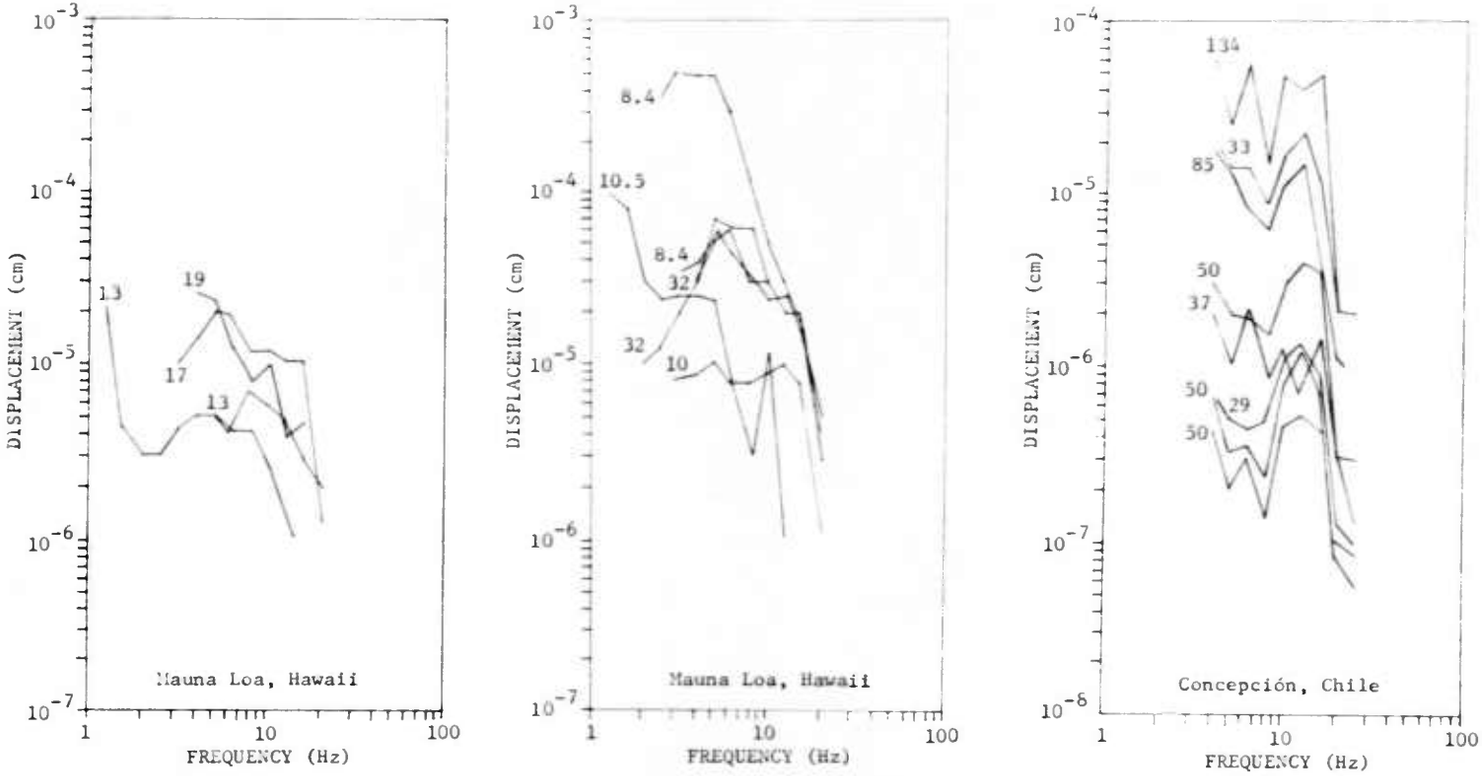

FIGURE 6. EARTHQUAKE CODA DISPLACEMENT SPECTRA NORMALIZED TO ZERO TIME. Shown are (S-P) distances in kilometers.

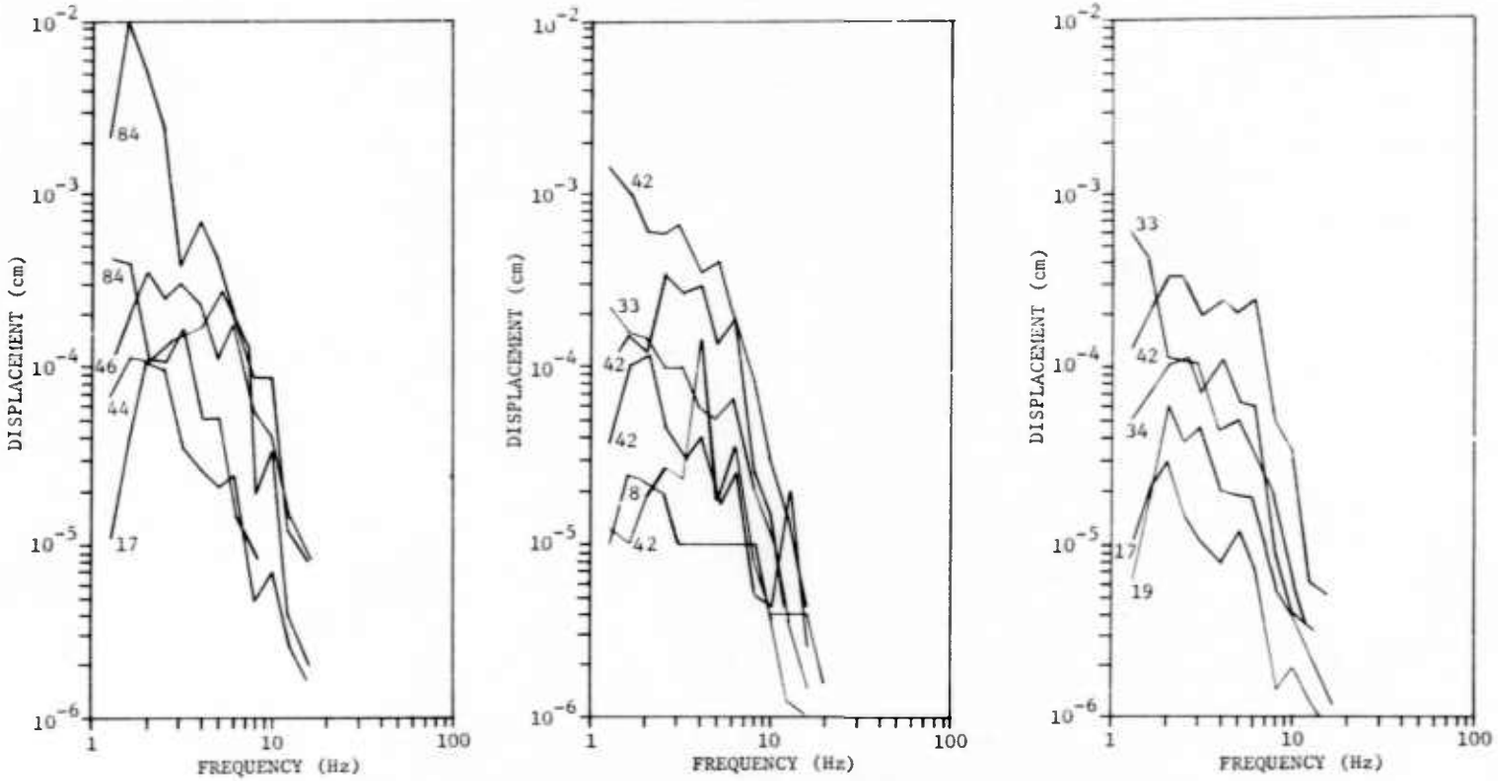

FIGURE 7. EARTHQUAKE CODA DISPLACEMENT SPECTRA RECORDED AT HOLLISTER, CALIFORNIA, 1961. Normalized to zero time. Shown are (S-P) distances in kilometers.

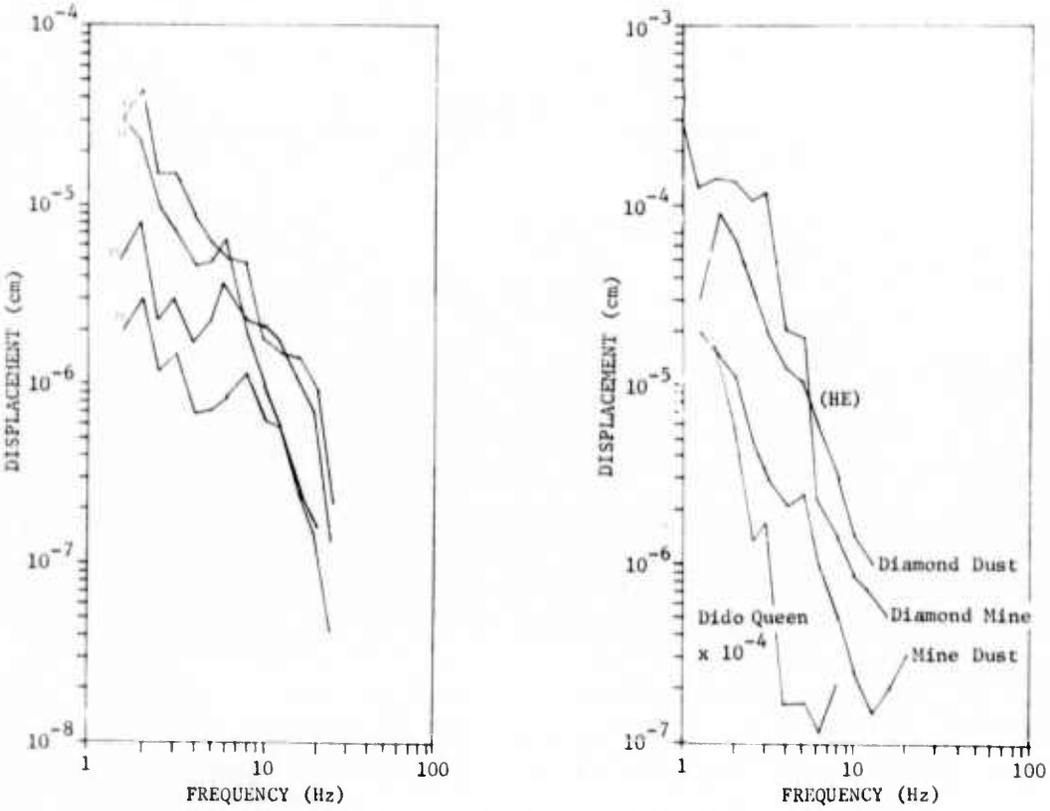

FIGURE 8. EXPLOSION CODA DISPLACEMENT SPECTRA RECORDED AT BERRY CREEK AND NTS, NEVADA. Normalized to zero time. Shown are (S-P) distances in kilometers.

TABLE 4. SOURCE PARAMETERS AS DETERMINED FROM CODA SPECTRAL ANALYSIS

Distance (km)	Local Magnitude	Characteristic Frequency (Hz)	Source Spectral Level (cm)
	Mauna Loa, Hawaii, 1962		
8.4	1.7	5.0	4.0×10^{-5}
8.4	2.5	5.0	4.0×10^{-4}
10.0	0.6	12.5	9.0×10^{-6}
10.5	0.5	<1.5	$>1.0 \times 10^{-4}$
13.0	0.6	8.0	5.0×10^{-6}
13.0	0.9	8.0	4.0×10^{-6}
17.0	1.2	5.0	1.5×10^{-5}
32.0	1.7	8.0	3.0×10^{-5}
32.0	2.0	6.0	5.0×10^{-5}
	Concepción, Chile, 1962		
29.0	0.3	12.5	1.2×10^{-6}
33.0	1.6	12.5	1.5×10^{-5}
37.0	1.0	16.0	1.2×10^{-6}
50.0	1.0	12.5	2.5×10^{-6}
50.0	-0.1*	12.5	5.5×10^{-7}
50.0	0.0*	12.5	3.0×10^{-7}
85.0	1.4	12.5	2.0×10^{-5}
134.0	1.9	16.0	4.0×10^{-5}
	Hollister, California, 1961		
8.0	1.5*	1.6	2.0×10^{-5}
17.0	0.8*	2.0	4.0×10^{-5}
17.0	1.0*	2.0	2.0×10^{-5}
19.0	1.7	2.0	2.5×10^{-5}
33.0	1.9	<1.5	$>7.0 \times 10^{-4}$
33.0	2.0	<1.5	$>3.0 \times 10^{-4}$
34.0	2.0	4.0	8.0×10^{-5}
42.0	1.4	2.0	7.0×10^{-5}
42.0	2.5	<1.5	$>3.0 \times 10^{-3}$
42.0	2.3	6.0	2.5×10^{-4}
42.0	2.1	4.0	2.0×10^{-4}
42.0	1.2	4.0	4.0×10^{-5}
44.0	1.6	5.0	2.0×10^{-4}
46.0	2.4	3.0	2.0×10^{-4}
84.0	2.1	<1.5	$>4.0 \times 10^{-4}$
84.0	2.0	1.6	5.0×10^{-3}

Table 4. (cont.)

Distance (km)	Local Magnitude	Characteristic Frequency (Hz)	Source Spectral Level (cm)
		NTS Explosions, 1970-1973	
6.0	1.5	3.0	3.0×10^{-4}
6.0	0.9	<1.3	$>2.0 \times 10^{-5}$
6.0	1.5	1.6	5.0×10^{-5}
12.0	4.6	<1.5	$>1.0 \times 10^{-1}$
		Mine Blasts Berry Creek, Nevada	
25.0	0.1	8.0	8.0×10^{-6}
25.0	0.7	2.0	3.0×10^{-6}
33.0	0.8	<2.0	$>4.5 \times 10^{-5}$
33.0	1.0	<2.0	$>3.0 \times 10^{-5}$

*Estimated from partially pinned recordings.

that the spectra implied by this model will be flat until a frequency related to the source dimension after which the level will fall off with frequency [17]. Randall has shown that the far-field results of Brune's model are not dependent on the dislocation model, and that the predicted spectra of Brune, Archembeau, and Randall agree well with observational spectra from microearthquakes [18].

In the Hanks and Thatcher graphical representation of the far-field displacement, three independent parameters are used to characterize the seismic source [19]. These are: the corner (characteristic) frequency, f_0; the long-period spectral level, Ω_0; and the measure of fractional stress drop, ε. Spectral characteristics such as f_0 and Ω_0 can be plotted on log-log paper for fixed ε. For a suite of earthquakes or explosions, comparisons can be made of the energy, magnitude, and stress drop if the functional dependence of these quantities on f_0 and Ω_0 is known.

Theoretically, the fractional stress drop has an important influence on the shape and Ω_0 level of the high frequency spectra. A value of ε less than unity will put a bend in the high frequency fall-off as well as lowering the observed value of Ω_0. These effects, however, cannot be determined from our data. When Ω_0 from the various coda spectra is plotted against the characteristic frequency, constant source dimension can be seen as a vertical trend. Likewise, constant moment is found as a horizontal trend. Magnitudes should increase uniformly with spectral level on this diagram. Earthquakes of constant stress drop lie along a line with slope equal to -3. Such a relationship is also predicted by Aki's ω^{-2} model.

---

17. Brune, J. N., Tectonic Stress and the Spectra of Seismic Shear Waves from Earthquakes, J. Geophys. Res., Vol. 75, 1970, pp. 4997-5009.

18. Randall, M. J., The Spectral Theory of Seismic Sources, Bull. Seism. Soc. Am., Vol. 63, No. 3, June 1973.

19. Hanks, T. C. and W. Thatcher, A Graphical Representation of Seismic Source Parameters, J. Geophys. Res., Vol. 77, August 1972, pp. 4393-4405.

In Fig. 9, Ω_0 and f_0 are plotted from the various code spectra. While showing strong regional effects, these data yield an ω^{-3} trend which suggests constant stress drop over this magnitude range. More specifically, the scatter is indicative of partial stress drop with constant source dimension which is especially true with the Chilean earthquakes. The scatter noted between sites suggests that discrimination must be treated on a regional basis. In addition, it does not appear that explosions can be discriminated from earthquakes at these magnitudes using high frequency spectra characteristics. The magnitudes tend to increase with the spectral level. These data are replotted in Fig. 10 to show the strength of M_L versus Ω_0 relationship. As obtained, Ω_0 is related directly to the apparent moment which is related to the local magnitude by

$$\text{Log}_{10} \text{ Moment} = 1.5\ M_L + C \quad [1]$$

This relationship describes the central trend of these data points.

The corner frequency (Hz) is nearly equal to the source dimension (km). A plot of local magnitude versus source dimension is given in Fig. 11. These data agree well with the central trend of those obtained by Wyss and Brune for California earthquakes where source dimensions were determined by a completely different method [3].

While these results agree with those obtained and predicted by other investigators, they do not define a threshold for M_s:m_b discrimination. The source characteristics plotted in Fig. 9 suggest that an m_b threshold for discrimination is greater than $m_b = 2$.

3.3. S-WAVE SPECTRUM ANALYSIS

The single largest problem in analyzing the spectra of body waves for source characteristics is accounting properly for path effects that change the earth's frequency response between source and station. The shape of high-frequency spectra is severely affected by attenuation varying with path depth. The mathematical form for seismic attenuation ϕ is usually given as:

$$\phi(f, r) = e^{-\frac{\pi f r}{Q V_s}}$$

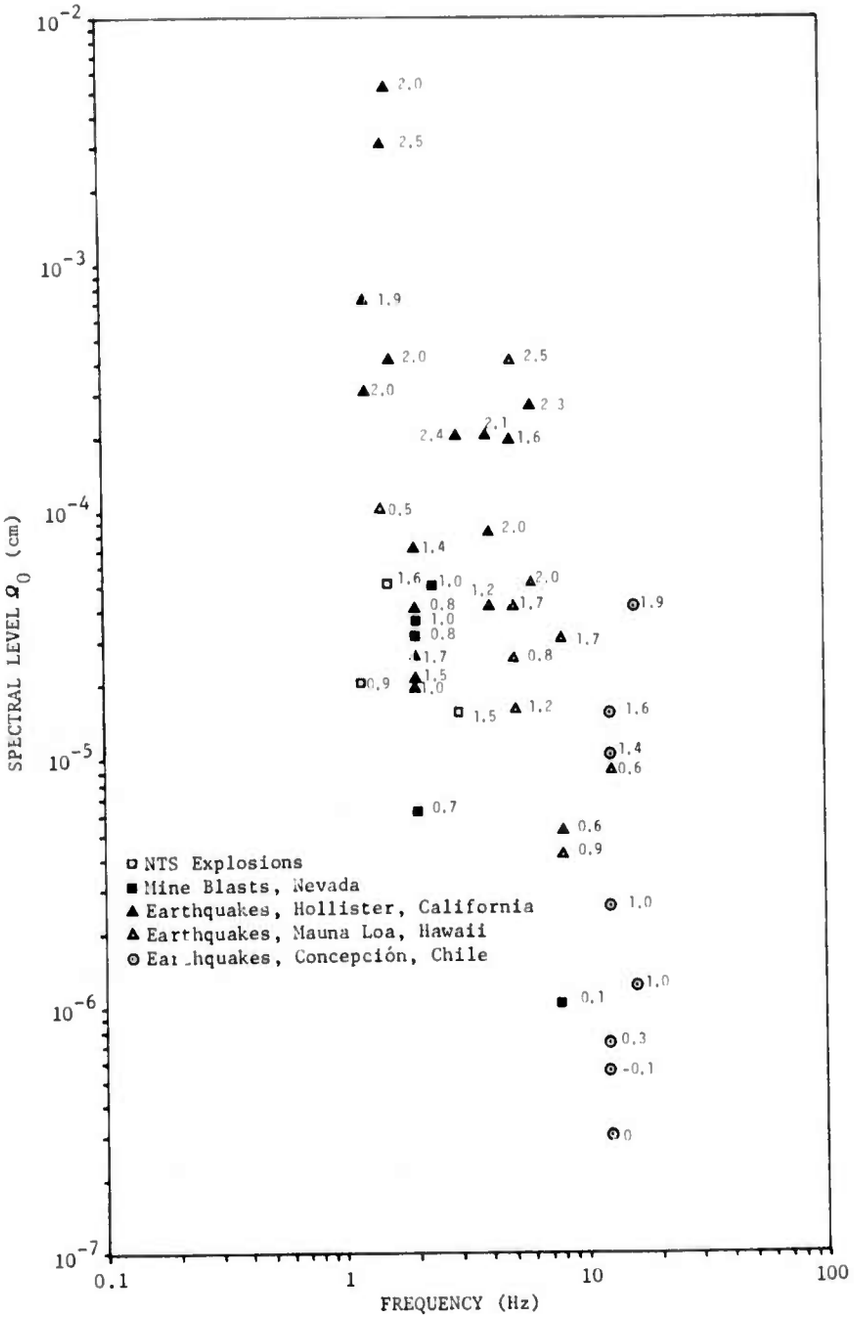

FIGURE 9. SOURCE SPECTRAL LEVEL VERSUS CHARACTERISTIC FREQUENCY. Shown are the local magnitudes M_L.

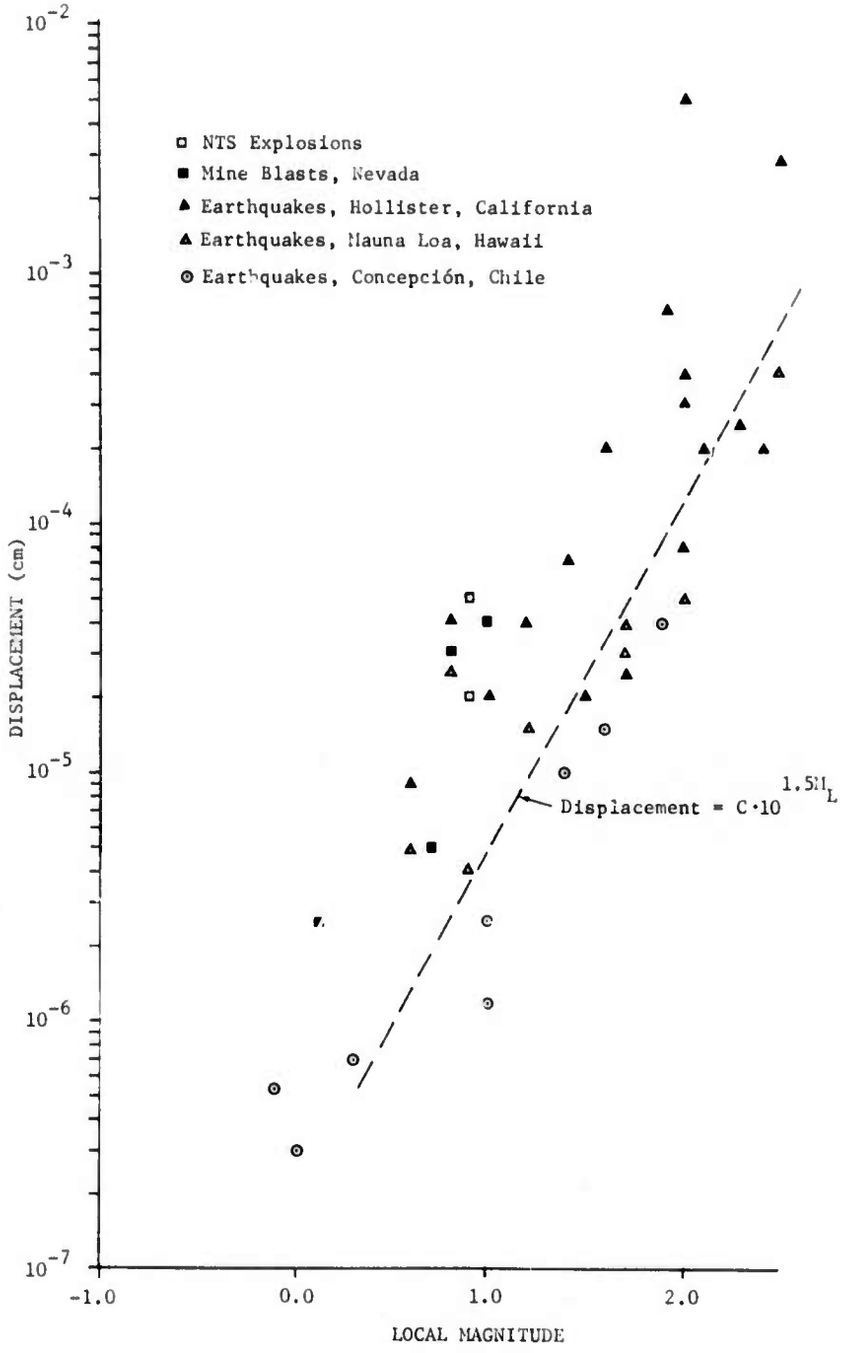

FIGURE 10. NORMALIZED CODA DISPLACEMENTS VERSUS LOCAL MAGNITUDE M_L

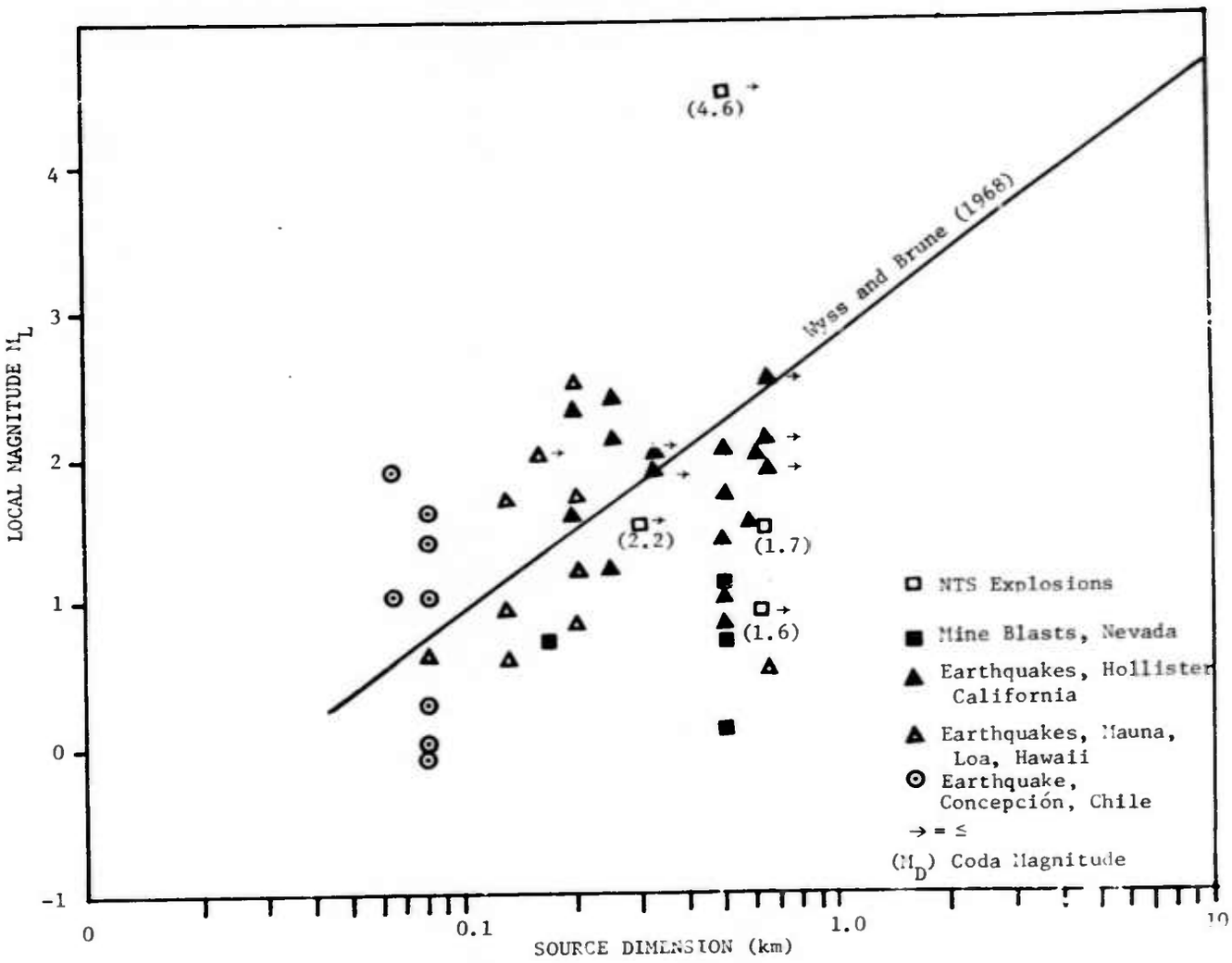

FIGURE 11. LOCAL MAGNITUDE VERSUS SOURCE DIMENSION

where f = frequency

r = distance in km

Q = absorption constant

V_s = wave velocity km/sec (of shear waves)

Q can be expected to increase with depth of wave penetration. For greater distances one would expect greater penetration and thus larger values of Q. If a shape for the source spectrum is assumed, the rough shape of the site spectrum can be calculated for various values of Q.

For a flat source displacement the effect on the particle velocity spectra is shown in Fig. 12. For convenience, station spectrums have been left in terms of particle velocity. All of the earlier spectral analysis was done in terms of particle velocity rather than displacement. The site particle velocity spectra for the flat displacements are of similar shape and vary in position according to the ratio of distance to Q. A pronounced effect is obtained if the source spectrum is assumed to be flat only to the characteristic frequency and then dominated by f^{-2} trend (see Savage [5]). The introduction of a spectral corner produces a peak in the station velocity spectra at the corner frequency.

In Fig. 13, cutoffs 1 through 4 give corresponding peak locations in the calculated velocity spectra. If the corner frequency is greater than the peak determined by Q for the flat spectra portion then the effect on velocity spectral shape is not pronounced. To obtain some idea where the corner frequency is located, the particle spectra of Fig. 13 can be fitted on field-measured spectra. Position of the Q-determined peak implies a value of Q if the distance is known.

If the test spectrum does not fit the cutoffs, a maximum Q and a minimum corner frequency are implied. This visual fitting technique has been applied to the maximum wave earthquake spectra for three separate locations. The maximum wave was considered in almost all cases to be a shear wave.

The approximated corner frequencies are plotted in Figs. 14, 15, and 16 with corresponding local magnitudes. Also shown are the implied Q and approximate range from S-P times. While a great degree of

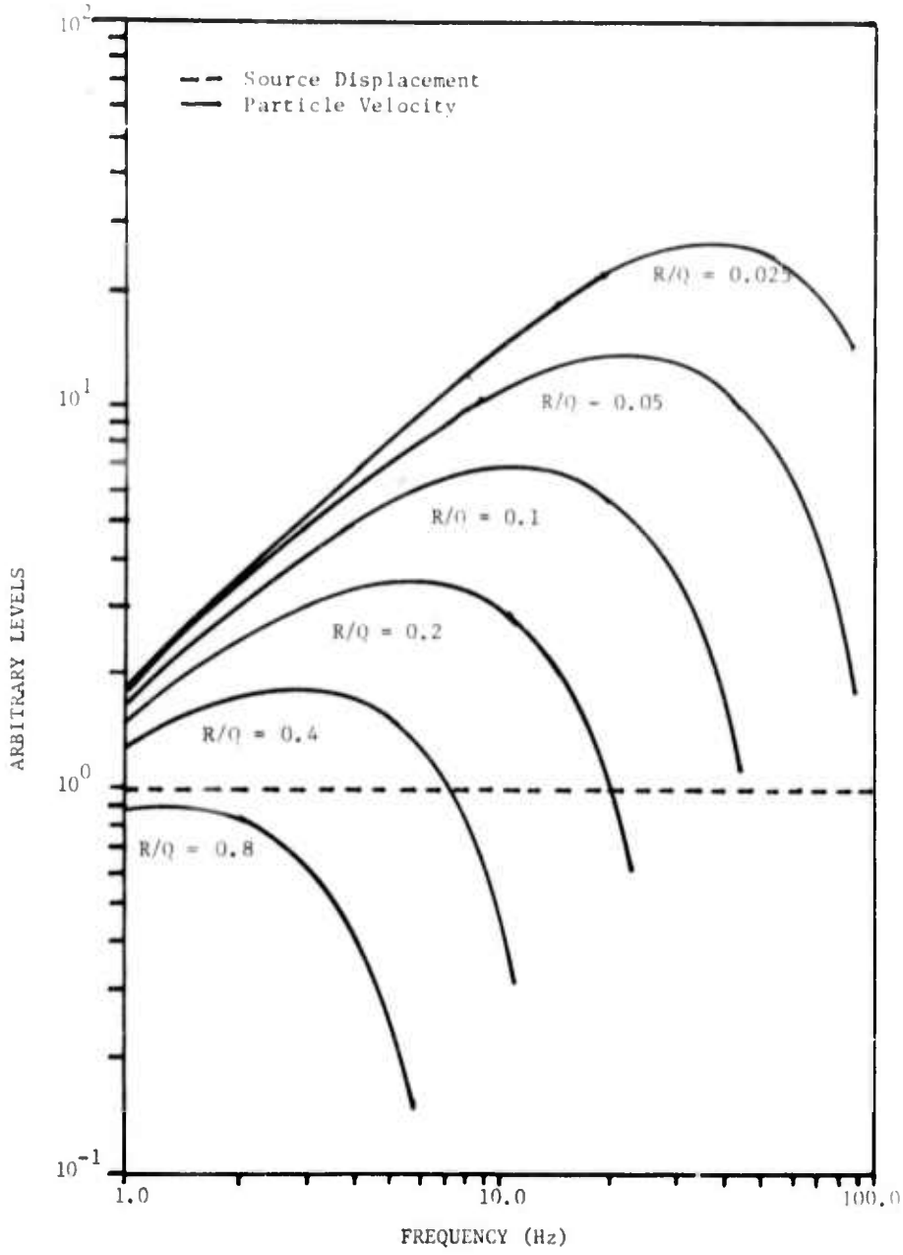

FIGURE 12. FLAT SOURCE DISPLACEMENT SPECTRA AND THEORETICAL PARTICLE VELOCITY SPECTRA FOR VARIOUS VALUES OF DISTANCE R/Q

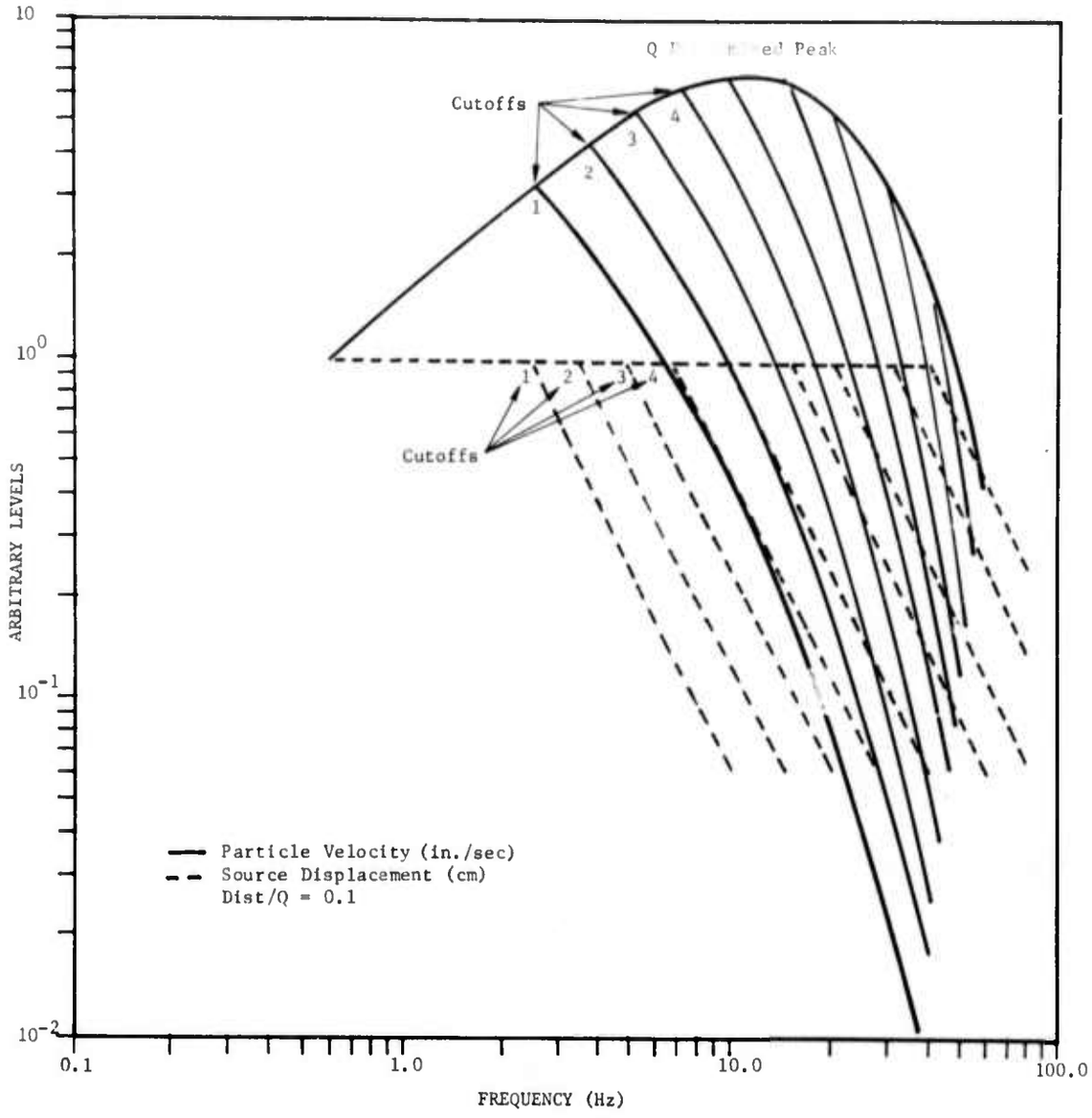

FIGURE 13. SOURCE DISPLACEMENT SPECTRA WITH ω^{-2} TREND AND CORRESPONDING PARTICLE VELOCITY SPECTRA WITH ATTENUATION CAUSED BY INTERNAL FRICTION

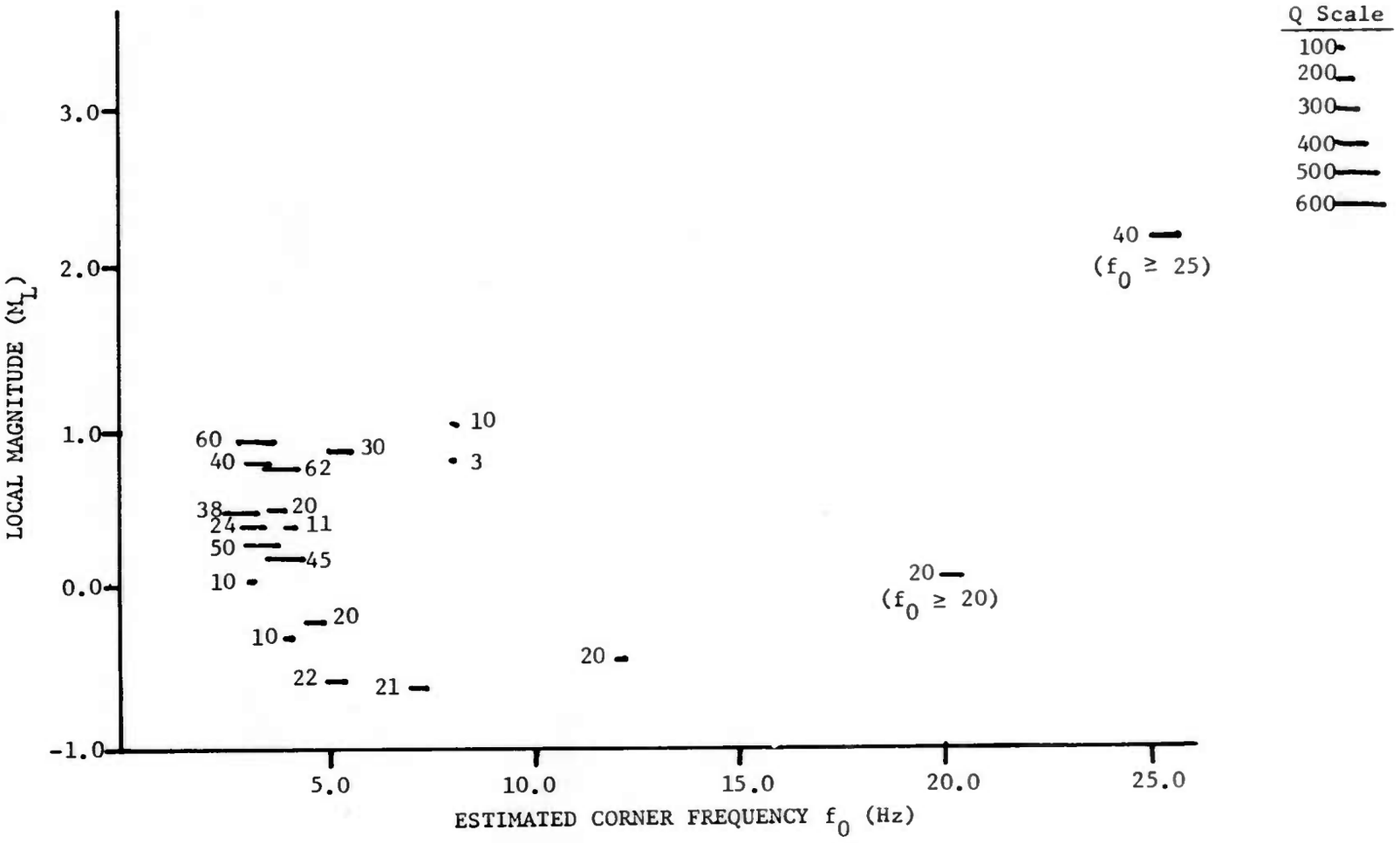

FIGURE 14. LOCAL EARTHQUAKE MAGNITUDE VERSUS ESTIMATED CORNER FREQUENCY OBTAINED AT MAXIMUM SIGNAL. Numbers represent approximate epicentral distance; lines, implied Q attenuation constant. Earthquakes recorded at Hollister, California.

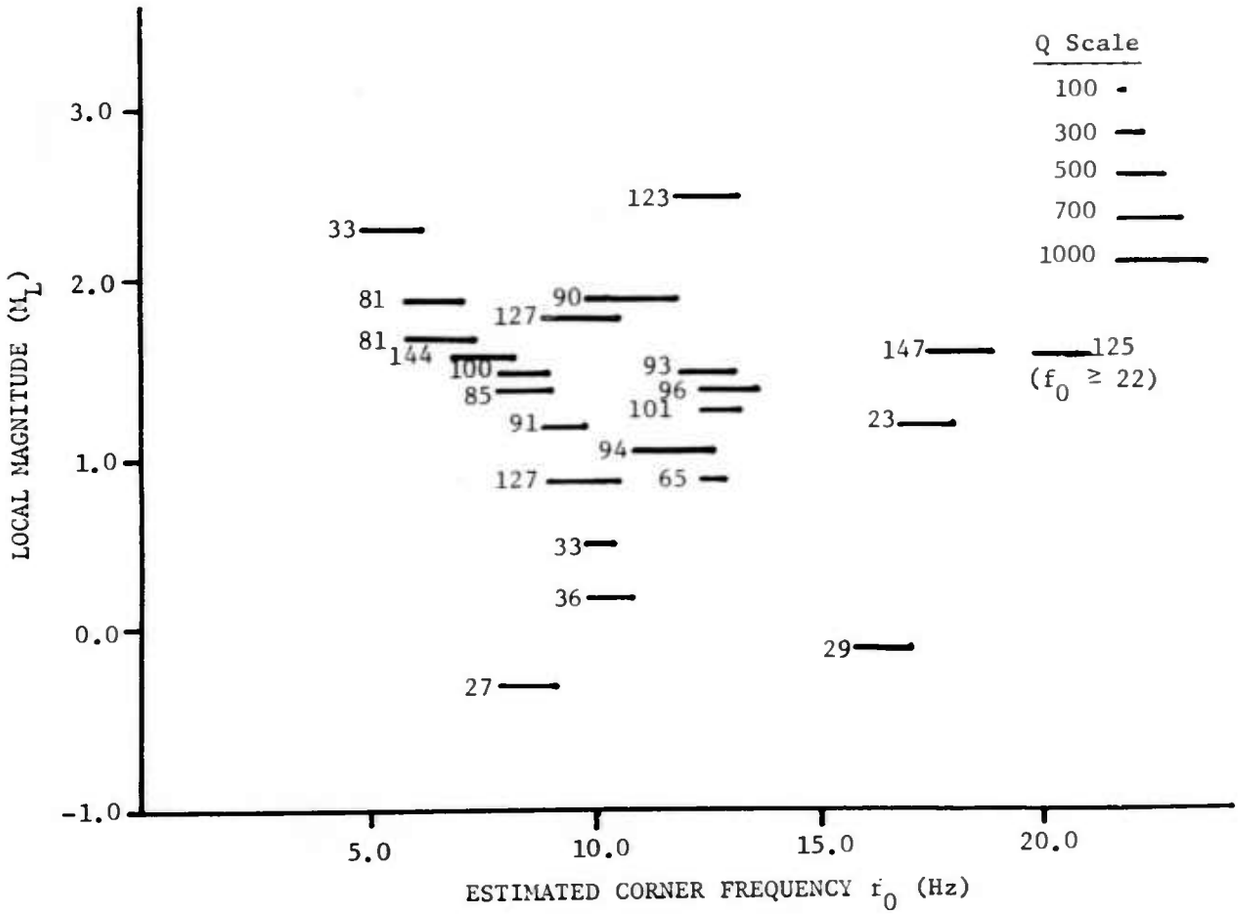

FIGURE 15. LOCAL EARTHQUAKE MAGNITUDE VERSUS ESTIMATED CORNER FREQUENCY OBTAINED AT THE MAXIMUM SIGNAL. Numbers represent approximate epicentral distance; lines, the implied Q attenuation constant. Earthquakes recorded at Mt. Laguna, California.

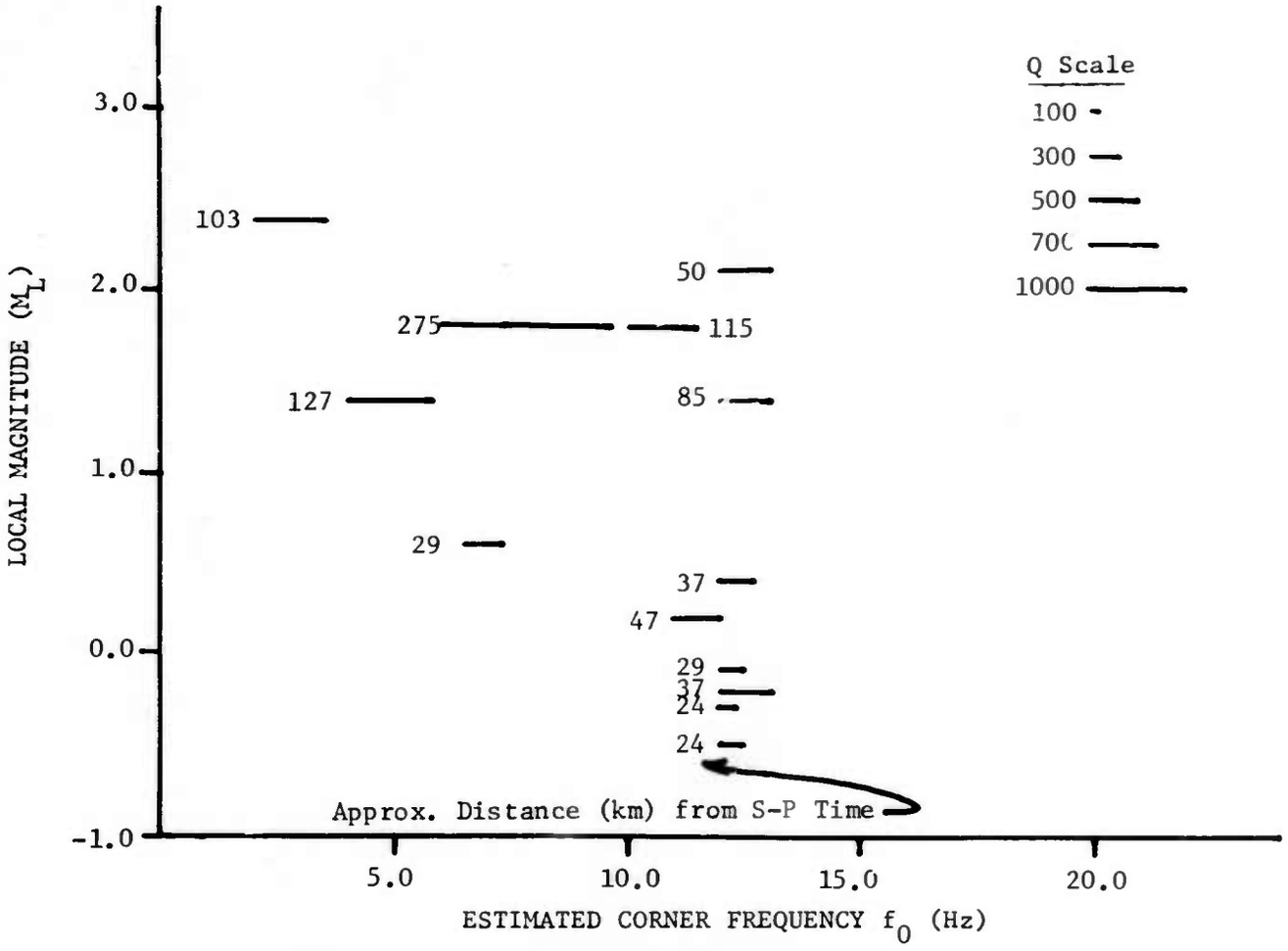

FIGURE 16. LOCAL EARTHQUAKE MAGNITUDE VERSUS ESTIMATED CORNER FREQUENCY OBTAINED AT THE MAXIMUM SIGNAL. Numbers represent approximate epicentral distance; lines, the implied Q attenuation constant. Earthquakes recorded at Concepción, Chile.

scatter is present, the results suggest that there are great differences between sites in the characteristic frequencies observed in the 1.0 to 3.0 magnitude range. While applying this technique to body waves produces corner frequencies which are fairly consistent with those obtained from coda analysis, the technique is considered much less reliable because of its subjective character. The scatter in Figs. 14, 15, and 16 is sufficient to eliminate this use of high frequency body wave spectra for explosion/earthquake discrimination. Furthermore, such scatter suggests that body wave path attenuation techniques cannot, as we have attempted here, be simply corrected.

4
CONCLUSIONS

Existing small earthquake data have been examined for characteristics which could be used for discrimination of earthquakes and explosions. Within the limits of high frequency spectra from these small earthquakes ($0 < M_L < 2.5$), no promising discriminants were found. Results suggest that the source time function cannot be used to discriminate earthquakes and explosions that are this small. Furthermore, most earthquakes and explosions examined showed corner frequencies higher than 1.0 Hz indicating that m_b would not work well as a discriminant in this magnitude range. Discrimination of explosions and earthquakes may be still possible on the basis of M_s.

While observed magnitude corner frequency relationship generally agreed with Aki's ω-squared model, a great amount of scatter occurred. Scatter can be attributed to the accuracy limitations of the technique, to variation in earthquake stress drop, and to strong regional effects.

Because of the presence of strong path effects, the use of observed high-frequency body wave spectra to obtain source information is not reliable unless substantial wave propagation effects are known.

The coda spectra analysis technique developed by Aki [1] was found useful in obtaining source spectral parameters from the coda frequency time spectrum. This coda technique could easily be adapted to the digital computer to achieve more rapid analysis. It is recommended that

further research be conducted using this approach but that application be made to earthquakes and explosion events of greater magnitude.

REFERENCES

1. Aki, K., Analysis of the Seismic Coda of Local Earthquakes as Scattered Waves, J. Geophys. Res., Vol. 74, No. 2, January 1969, pp. 614-631.

2. Aki, K., Scaling Law of Earthquake Source Time-Function, Geophys. Journal Roy. Astro. Soc., Vol. 31, December 1972, pp. 3-25.

3. Wyss, M. and J. N. Brune, Seismic Moment, Stress, and Source Dimensions for Earthquakes in the California-Nevada Region, J. Geophys. Res., Vol. 73, No. 14, July 1968, pp. 4681-4694

4. SIPRI, Seismic Methods for Monitoring Underground Explosions, Stockholm International Peace Research Institute, Ed., D. Davies, 1971.

5. Savage, J. C., Relation of Corner Frequency to Fault Dimensions, J. Geophys. Res., Vol. 77, No. 20, July 1972, pp. 3788-3795.

6. Aki, K., Theoretical $M_s - m_b$ Relation for Small Magnitudes, Woods Hole Conference on Seismic Discrimination, Ed., J. F. Evernden, Vol. 1, July 1970, pp. 57-70.

7. Aki, K., and Tsai, Y-B, Amplitude Spectra of Surface Waves from Small Earthquakes and Underground Nuclear Explosions, Woods Hole Conference on Seismic Discrimination, Ed., J. F. Evernden, Vol. 1, July 1970, pp. 291-328.

8. Thirlaway, H. I. S., SIPRI, Seismic Methods for Monitoring Underground Explosions, Stockholm International Peace Research Institute, 1968, p. 63.

9. Basham, P. W., SIPRI, Seismic Methods for Monitoring Underground Explosions, Stockholm International Peace Research Institute, 1968, p. 67.

10. Richter, C. F., An Instrumental Magnitude Scale, Bull. Seism. Soc. Am., Vol. 25, 1935, pp. 1-32.

11. Tanis, F. J., High-Frequency Spectra of Earthquakes and Explosions, Semi-Annual Informal Technical Report Number 192700-2-T, Environmental Research Institute of Michigan, Ann Arbor, February 1973.

12. Bayer, K. C. and G. M. Wuollet, A Magnitude Yield Evaluation of Nuclear Events and One Chemical Explosion on the Nevada Test Site, U.S.G.S. Unpublished Report, July 1973.

13. Clark, S. P., Ed., Handbook of Physical Constants, Geological Society of America, Memoir 97, 1966.

14. Randall, M. J., Seismic Radiation from a Sudden Phase Transition, J. Geophys. Res., Vol. 71, 1966, pp. 5297-5302.

15. Archembeau, C. B., General Theory of Elastodynamic Source Fields, Review of Geophysics, Vol. 6, 1968, pp. 241-287.

16. Randall, M. J., Spectral Peaks and Earthquake Source Dimension, J. Geophys. Res., Vol. 78, No. 14, May 10, 1973, pp. 2609-2611.

17. Brune, J. N., Tectonic Stress and the Spectra of Seismic Shear Waves from Earthquakes, J. Geophys. Res., Vol. 75, 1970, pp. 4997-5009.

18. Randall, M. J., The Spectral Theory of Seismic Sources, Bull. Seism. Soc. Am., Vol. 63, No. 3, June 1973, pp. 1133-1144.

19. Hanks, T. C. and W. Thatcher, A Graphical Representation of Seismic Source Parameters, J. Geophys. Res., Vol. 77, August 1972, pp. 4393-4405.